North Western Mussels Spat Nursery
Proposed Waikato West Coast Mussel Nursery

Assessment of potential impact on hydrodynamic conditions

Report prepared for North Western Mussels Limited

November 2022

MetOcean SOLUTIONS

Document History

Versions

Version	Revision Date	Summary	Reviewed by
0.1	3/10/2022	Initial document created	Sorensen
0.2	7/10/2022	Draft for internal review	Sorensen
0.3	9/10/2022	Draft for internal review	Sorensen
0.4	12/10/2022	Draft for internal review	Thiebaut
0.5	13/10/2022	Draft for internal review	Berthot
0.6	17/10/2022	Draft for internal review	Sorensen
0.7	17/10/2022	Draft for client review	Berthot
0.8	08/11/2022	Revised draft for client review	Sorensen/Berthot

Distribution

Version	Date	Distribution
1.0	08/11/2022	North Western Mussels Limited
2.0	17/11/2022	North Western Mussels Limited

Document ID: P0589 - 01

Authors

Sorensen S., Thiebaut S., Berthot A.,

Contributors

MetOcean Solutions is a Division of Meteorological Services of New Zealand Ltd, MetraWeather (Australia) Pty Ltd [ACN 126 850 904], MetraWeather (UK) Ltd [No. 04833498] and MetraWeather (Thailand) Ltd [No. 0105558115059] are wholly owned subsidiaries of Meteorological Service of New Zealand Ltd (MetService).

must not be disclosed to any third person without the prior written approval of Meteorological Service of New Zealand Ltd. Meteorological Service of New Zealand Ltd

Contents

List of Figures

List of Tables

1. Introduction

1.1 Scope of Report

North Western Mussels Limited (NWML) is planning to apply for a resource consent to undertake green lipped mussel (*Perna canaliculus*) spat collection and nursery activities off the west coast of Waikato. NWML have asked MetOcean Solutions to provide a summary of hydrodynamic conditions at the proposed spat nursery sites and assess the potential effects of the spat collection and nursery activities on the hydrodynamics.

The concept of the west coast nursery is that some spat will be relocated at a small size on the catching ropes while others will be held on the west coast to final seed average size of 70mm, harvested and final seeded into the Hauraki Gulf. Some lines may be seeded with hatchery spat for the nursery phase, again prior to final seeding at an average of 70mm into the Hauraki Gulf. The strategy is aimed at spreading the range of spat collection and retention risks over a range of sources and locations.

This study is based on literature review and modelled data and aims to investigate the potential effects of the four proposed mussel spat nursery sites (Figure 1-1 and Appendix A) on waves, current attenuation, and erosion of adjoining foreshore, surf breaks, and as such, the natural state of the hydrodynamic conditions.

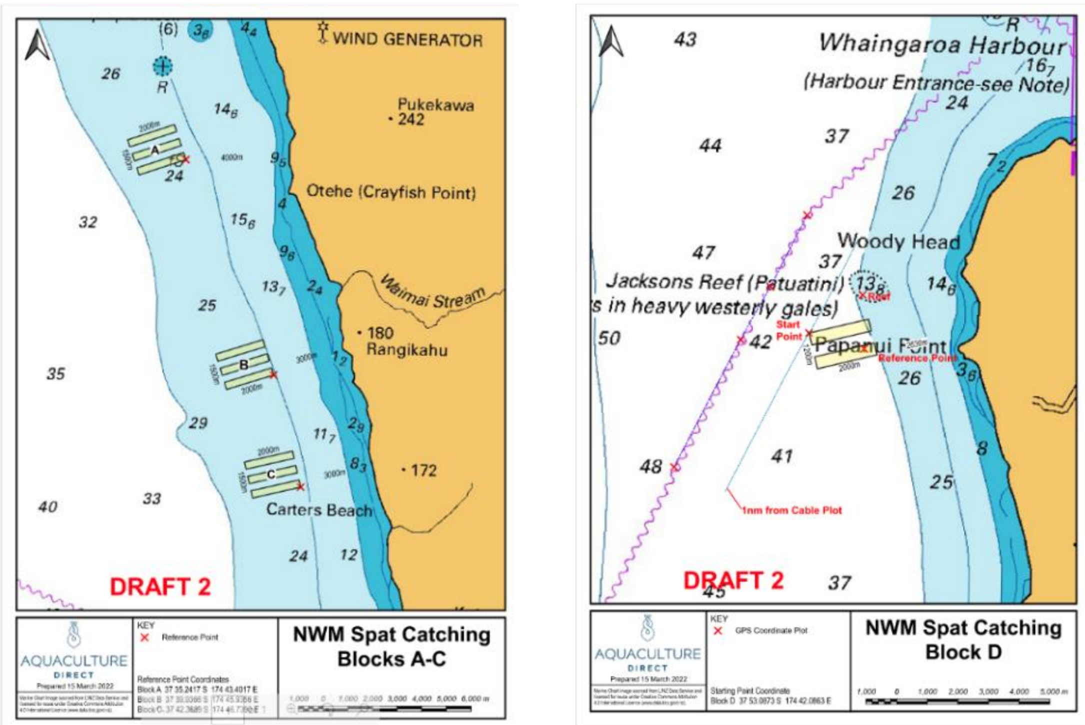

Figure 1-1. Locations of the four proposed mussel nursery sites (sites A, B, C and D) and rows on the Waikato west coast.

1.2 Outline of Activities

The aim of the west coast nursery is to serve as a donor site of spat to commercial mussel farms in the Hauraki Gulf. This will allow to spread the risks that mussel spat are subjected to at various life stages and environments (i.e. mussel spat are then collected by different strategies and at different geographical locations).

Four sites (Site A, B, C and D) have been proposed by the applicant for mussel spat nursery. The sites are between 3 to 4 km from the shoreline and in water depths ranging between 20 to 40 m. The two most distant sites (Site A and D) are approximately 32 km apart (see Figure 1.1). Site A, B and C will consist of three rows, and Site D consist of two rows. The rows at Site A, B and C will measure 300 m x 2000 m, whereas, the rows at Site D will measure 400 m x 2000 m. The reason the rows on Site D are wider is that the seabed is deeper at site D so a longer total longline is required to achieve a similar length of backbone.

The combined area will cover 700 hectares (see table 1-1).

Table 1-1. The combined area covered by proposed west coast nursery including unoccupied area between lines and rows.

	Site A	**Site B**	**Site C**	**Site D**	**Total**
Row 1	60ha	60ha	60ha	80ha	
Row 2	60ha	60ha	60ha	80ha	
Row 3	60ha	60ha	60ha		
Total consented area	180ha	180ha	180ha	160ha	**700ha**

Each row will consist of single or paired lines which will be anchored by screw anchors 6 to 12 m deep in the seafloor (Figure 1-2). The backbones will run the width of each row at a distance of 50 m apart, ie there will be 41 x 300 m longlines per row running down the 300 m row length for Sites A, B and C, and for Site D, 41 x 400 m longlines per row running down the 400 m row length (see Figure 1-3 and Figure 1-4). Most mussel farms have longline spacings of 15 to 20 m apart but the increased distance of 50 m is a response to the open ocean conditions at the sites.

Close to surface length of the longline (the backbone) may vary from 130m to 150 depending on the depth on each site, and about 75m of warp between the anchor point and the longline will be used at either end of the longline. The warp will be longer at the deeper site D.

On the 150m longline backbone the catching rope (dropper lines) will go down 8m and up 8m once every 0.5 m, so this amount to 4 droppers or 32m of catching rope every 1m of backbone. Considering that this setup will be repeated over 150m of long line and for

41 longlines covering the 2000m row, the droppers line density (or number of droppers per square metre) will be approximately 0.041 dropper.m^{-2} for each row of Block A.B.C (over 60 ha) and 0.031 dropper.m^{-2} for each row of Block D (over 80ha). If a whole block (A, B, C or D) is considered the dropper density is then reduced as each row is separated by 300m.

Should paired lines be used, which may be considered for 50% of the site (i.e. 50% with double lines and 50% with single lines) the dropper density would increase to 0.082 dropper.m^{-2} for the area where double lines are used (Block A, B, C).

The backbone will be suspended 3 m below the sea surface by 20 floats/buoys of 300 litres each. The spacing of the floats will vary with time and weight on the line but is typically expected to start at 10 m apart and increase to 2m with time and weight.

Waikato West Coast Mussel Spat Catching and Nursary Long Line Structure

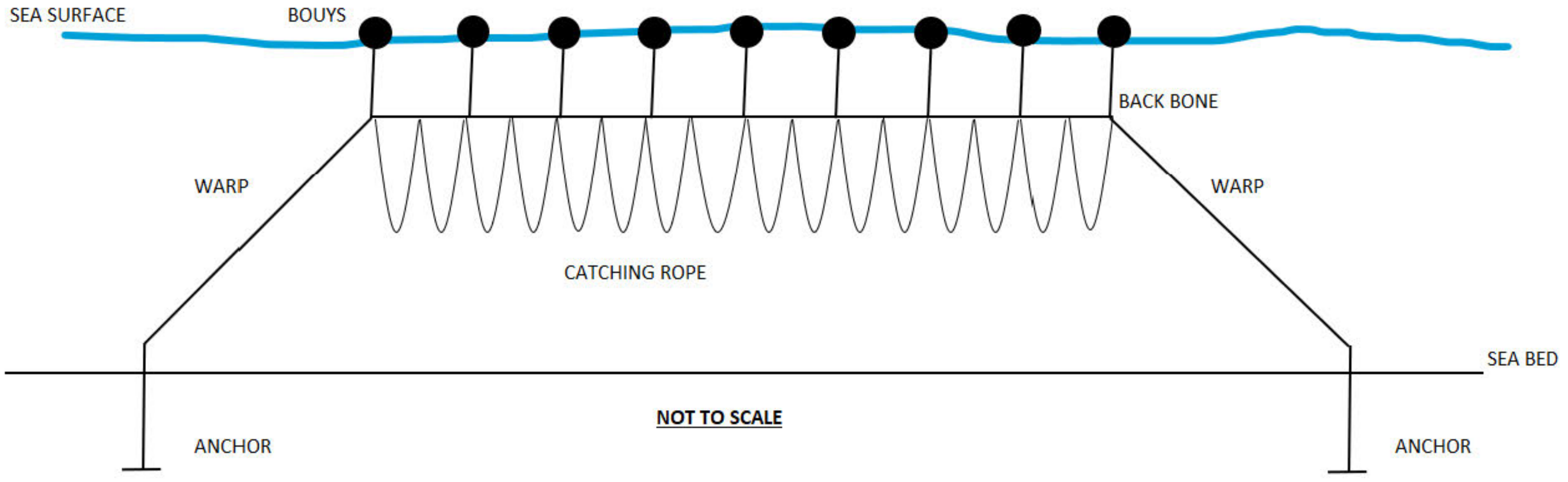

Anchors:	To be drilled into the seabed 6m - 12m depending on site substrate
Warps:	To be 32mm to 44mm diameter rope with 30ton plus breaking strain
Buoys:	Spaced 2m to 10m apart
Backbone:	150m in length and 32mm diameter
Catching rope:	8m down in length. 60mm-80mm diameter weighted fribulated self tensioning catching rope

Figure 1-2. Diagram illustrating an example of potential long line with dropper lines arrangement.

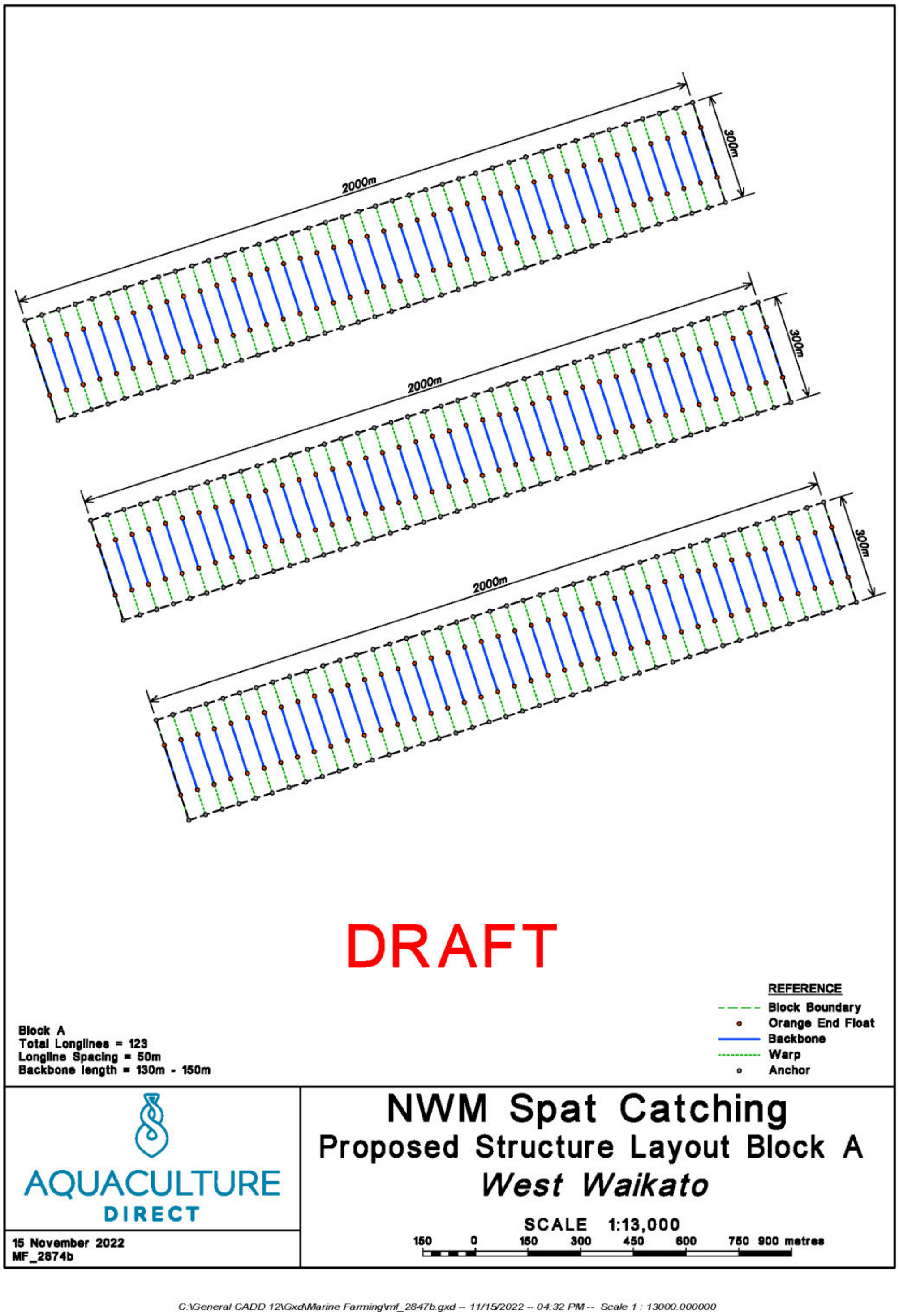

Figure 1-3. Proposed Structure layout for Block A .

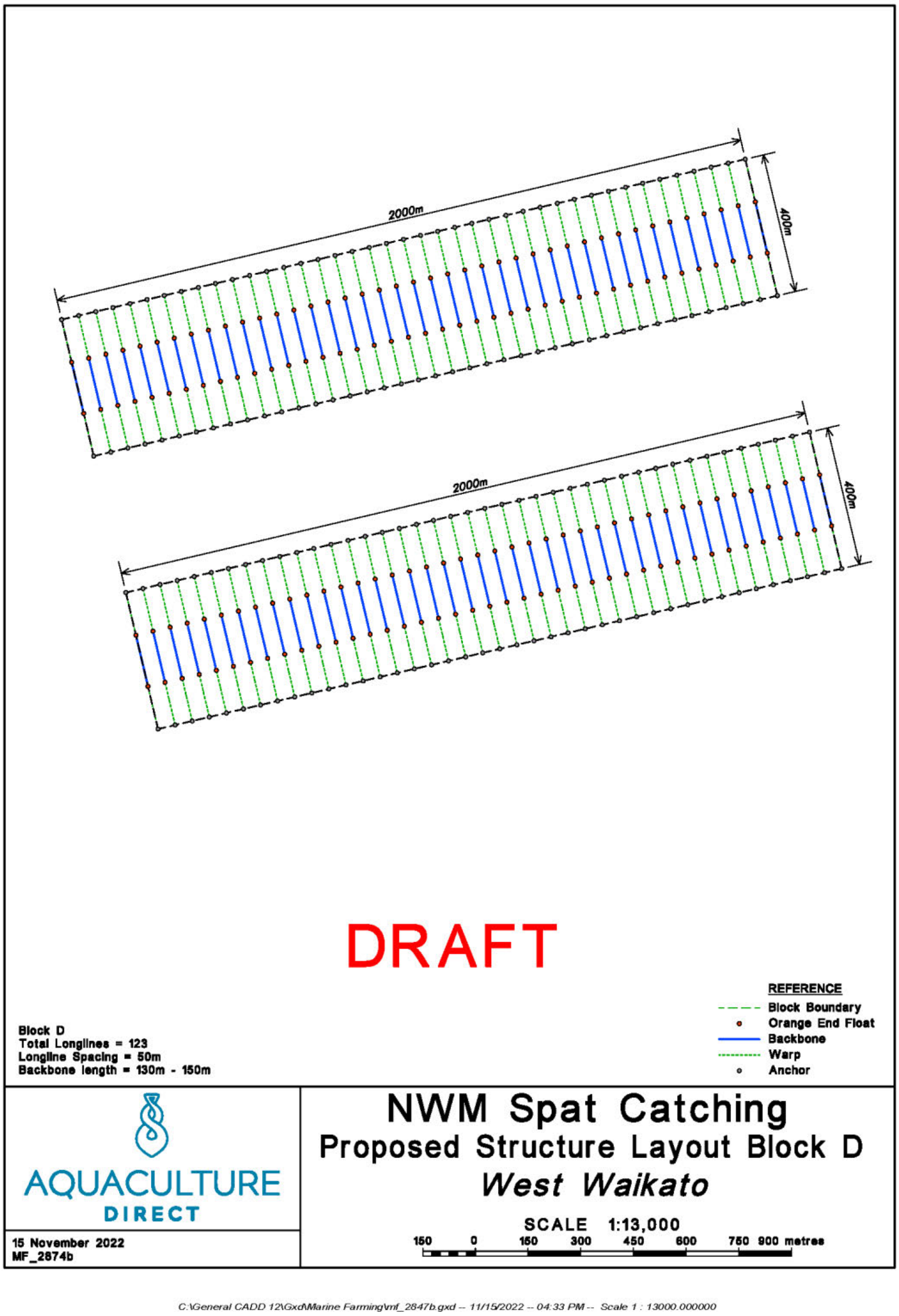

Figure 1-4. Proposed Structure layout for Block D.

The catching rope has a filamentous surface (60 to 80 mm long "hairs"), which acts as a favourable settlement surface for the microscopic free-swimming larvae. Post settlement, the larvae will undergo metamorphosis from larvae to adult (Figure 1-5).

Figure 1-5. Spat catching rope post settlement and metamorphosis of wild green lipped mussel (Perna canaliculus) spat (Source: S. Sorensen 2022)

Mussel spat collection for research purposes conducted by NWML at the proposed locations, found that autumn catch is 60% reliable and the winter and spring catch 100% reliable. As such, the spat will be caught between February and November, and harvested as required. Harvest and relocation of spat will occur at the three following stages:

- Spat is just visible (on rope).
- Spat on grown up to 20 mm (on rope)
- Spat average of 70 mm (spat stripped off rope)

Mussels will then be relocated from the west coast nursery and on-grown in farms in the Hauraki Gulf to a final harvest size of 95 to 105 mm.

The spat catching operations are intended to be seasonal (principally winter and spring) but the nursery activities will be carried out all year around. Harvesting of the spat/seed ropes from sites A to D will occur as required, but generally fortnightly, with maintenance carried out as part of these visits. If there are times where the spat/seed operation is not active, maintenance will be carried out through 2-day monthly visits to assess the structural integrity and rectify any wear and tear on lines, buoys, and lighting.

To aid maritime navigation, marker buoys with yellow flashing lights will be placed 200 m outside the nursery sites, or as required by Maritime NZ and/or WRC. In addition, orange marker buoys will also be placed at the end of each backbone and one central marker buoy outside the longlines, or as required by Maritime NZ and/or WRC.

2. Site Conditions

Hydrodynamic conditions and wave climate at the four mussel spat collection sites are assessed by statistical analysis of the following MetOcean Solutions hindcast datasets: NZ Wind (WRF), Moana 3D (ROMS) and NZ Wave North Island (SWAN). Details of each model are provided in Appendix A (Section 6). Analytical methods to calculate wave parameters from the modelled spectra are provided in Appendix B (Section 7). Statistical analyses are presented separately for each of the four sites in this section.

Data representing site conditions are extracted from the nearest domain node using the coordinates from the SouthWest (SW) corners of each block (Table 2-1).

Table 2-1 Site/Block coordinates.

Block	Corner	Northing (NZTM)	Easting (NZTM)	Latitude S (WGS-84 DDM)	Longitude E (WGS-84 DDM)
A	NW	1749789	5839373	174 41.7838 E	37 34.8306 S
	NE	1751690	5839995	174 43.0673 E	37 34.4757 S
	SE	1752156	5838570	174 43.4015 E	37 35.2414 S
	SW	1750255	5837948	174 42.1178 E	37 35.5964 S
B	NW	1753370	5830665	174 44.3257 E	37 39.5025 S
	NE	1755282	5831252	174 45.6182 E	37 39.1659 S
	SE	1755722	5829818	174 45.9357 E	37 39.9365 S
	SW	1753810	5829231	174 44.6430 E	37 40.2732 S
C	NW	1754536	5826283	174 45.1742 E	37 41.8594 S
	NE	1756486	5826724	174 46.4951 E	37 41.6012 S
	SE	1756817	5825260	174 46.7392 E	37 42.3891 S
	SW	1754866	5824820	174 45.4174 E	37 42.6469 S
D	NW	1749620	5805603	174 42.0859 E	37 53.0870 S
	NE	1751567	5806060	174 43.4081 E	37 52.8207 S
	SE	1751842	5804892	174 43.6104 E	37 53.4493 S
	SW	1749895	5804434	174 42.2881 E	37 53.7162 S

2.1 Site A

Wave data was extracted from the nearest model node at -37.56°S, 174.68°E, and current data from the nearest model node 37.5629°S, 174.6927°E. The predominant direction of the spectral peak is from SW (probability = 66.2%) with the most frequently encountered significant wave heights ranging between 1.0 to 1.5 m from SW (probability = 19.7%, Figure 2-1 and Table 2-2).

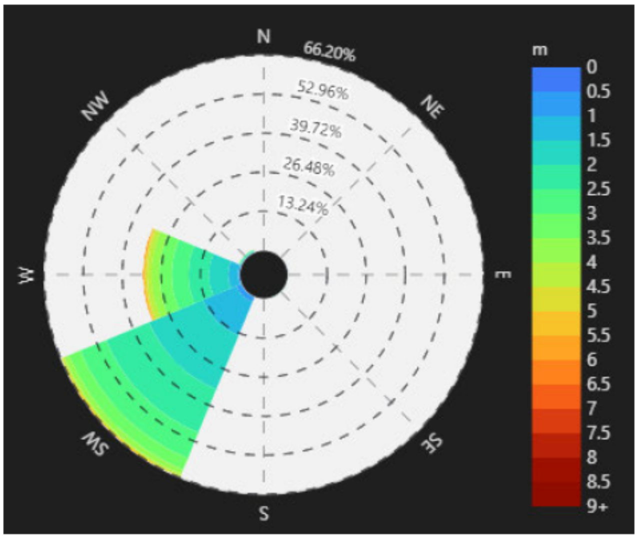

Figure 2-1 Wave rose for the proposed locations of the mussel spat collection Site A.

Table 2-2 Significant wave height and mean direction of spectral peak joint probability (%) for mussel spat nursery Site A.

Wave height / Wave direction	N	NE	E	SE	S	SW	W	NW
0 - 0.5	0%	0%	0%	0%	0%	<0.1%	<0.1%	0%
0.5 - 1	<0.1%	<0.1%	<0.1%	0%	<0.1%	1.80%	0.50%	<0.1%
1 - 1.5	<0.1%	<0.1%	<0.1%	<0.1%	<0.1%	12.40%	3.20%	0.20%
1.5 - 2	<0.1%	<0.1%	<0.1%	<0.1%	<0.1%	19.70%	6.50%	0.30%
2 - 2.5	0%	0%	<0.1%	<0.1%	<0.1%	15.90%	7%	0.30%
2.5 - 3	0%	0%	0%	0%	<0.1%	9.40%	5.50%	0.10%
3 - 3.5	0%	0%	0%	0%	0%	4.20%	4.20%	<0.1%
3.5 - 4	0%	0%	0%	0%	0%	1.70%	2.70%	<0.1%
4 - 4.5	0%	0%	0%	0%	0%	0.70%	1.50%	<0.1%
4.5 - 5	0%	0%	0%	0%	0%	0.30%	0.70%	0%
5 - 5.5	0%	0%	0%	0%	0%	0.10%	0.40%	<0.1%
5.5 - 6	0%	0%	0%	0%	0%	<0.1%	0.20%	0%
6 - 6.5	0%	0%	0%	0%	0%	<0.1%	<0.1%	0%
6.5 - 7	0%	0%	0%	0%	0%	<0.1%	<0.1%	0%
7 - 7.5	0%	0%	0%	0%	0%	0%	<0.1%	0%
7.5 - 8	0%	0%	0%	0%	0%	0%	<0.1%	0%
8 - 8.5	0%	0%	0%	0%	0%	0%	<0.1%	0%
8.5 - 9	0%	0%	0%	0%	0%	0%	<0.1%	0%

A joint probability analysis of significant wave height and relative peak period indicates that relative peak period (smooth) most frequently range between 11 to 17 seconds with significant wave heights of 1 to 3.5 m (Table 2-3).

Table 2-3 Significant wave height (m) and relative peak period (smooth) joint probability (%) for mussel spat nursery Site A.

wave height (m) \ peak period (sec)	**0 - 1**	**1-2**	**2-3**	**3-4**	**4-5**	**5-6**	**6-7**	**7-8**	**8-9**	**9-10**	**10-11**	**11-12**	**12-13**	**13-14**	**14-15**	**15-16**	**16 - 17**	**17 - 18**	**18 - 19**	**19 - 20**
0 - 0.5	0	0	0	0	0	0	0	0	0	0	<0.1	<0.1	<0.1	<0.1	0	0	0	<0.1	<0.1	0
0.5 - 1	0	0	0	<0.1	<0.1	<0.1	0	<0.1	<0.1	<0.1	0.10	0.40	0.60	0.40	0.20	0.20	0.10	<0.1	<0.1	<0.1
1 - 1.5	0	0	0	<0.1	<0.1	<0.1	<0.1	0.10	0.20	0.20	0.60	2.30	4	3.70	1.90	1.10	0.80	0.20	0.30	<0.1
1.5 - 2	0	0	0	0	<0.1	<0.1	0.20	0.30	0.50	0.60	0.90	2.50	5.50	6.80	4.10	2.40	1.60	0.40	0.50	0.20
2 - 2.5	0	0	0	0	<0.1	<0.1	0.10	0.40	0.60	0.60	1	1.70	3.50	5.50	4.50	2.60	1.70	0.40	0.40	0.10
2.5 - 3	0	0	0	0	0	0	<0.1	0.30	0.50	0.50	0.60	1.10	2	3.20	3.10	2.10	1.20	0.30	0.20	<0.1
3 - 3.5	0	0	0	0	0	0	<0.1	<0.1	0.40	0.40	0.40	0.50	1	1.60	1.60	1.30	0.90	0.20	0.10	<0.1
3.5 - 4	0	0	0	0	0	0	0	<0.1	0.10	0.30	0.20	0.30	0.50	0.80	0.80	0.70	0.60	0.20	<0.1	<0.1
4 - 4.5	0	0	0	0	0	0	0	0	<0.1	0.10	0.10	0.20	0.20	0.30	0.40	0.30	0.30	<0.1	<0.1	<0.1
4.5 - 5	0	0	0	0	0	0	0	0	<0.1	<0.1	0.10	0.10	0.10	0.20	0.20	0.10	0.10	<0.1	<0.1	<0.1
5 - 5.5	0	0	0	0	0	0	0	0	0	<0.1	<0.1	<0.1	<0.1	<0.1	0.10	<0.1	<0.1	<0.1	<0.1	0
5.5 - 6	0	0	0	0	0	0	0	0	0	0	<0.1	<0.1	<0.1	<0.1	<0.1	<0.1	<0.1	<0.1	<0.1	0
6 - 6.5	0	0	0	0	0	0	0	0	0	0	0	<0.1	<0.1	<0.1	<0.1	<0.1	<0.1	<0.1	<0.1	0
6.5 - 7	0	0	0	0	0	0	0	0	0	0	0	<0.1	<0.1	<0.1	<0.1	<0.1	<0.1	0	0	0
7 - 7.5	0	0	0	0	0	0	0	0	0	0	0	0	0	<0.1	<0.1	0	<0.1	0	0	0
7.5 - 8	0	0	0	0	0	0	0	0	0	0	0	0	0	<0.1	0	0	0	0	0	0
8 - 8.5	0	0	0	0	0	0	0	0	0	0	0	0	0	0	<0.1	0	<0.1	0	0	0
8.5 - 9	0	0	0	0	0	0	0	0	0	0	0	0	0	0	0	<0.1	0	0	0	0

An extreme value analysis indicates that a 1-year return period storm event (which has a likelihood of being equalled or exceeded of 63.2% in any one year) has 7.2 m significant wave height and 30 m/s average winds speeds (Table A 4).

Table 2-4 Extreme analysis of wave and wind conditions at Site A.

Return period [years]	**1**	**5**	**10**	**50**	**100**	**1000**	**10000**
Significant wave height (m)	7.2	8.0	8.4	9.1	9.5	10.6	11.7
Wind speed (m/s)	30	34.7	36.7	41.5	43.6	50.7	57.9

The predominant current direction is N-NW to SE (Figure A-4), with the highest probability current direction being from a NW to N sector (20.8.4% probability, Table A-4).

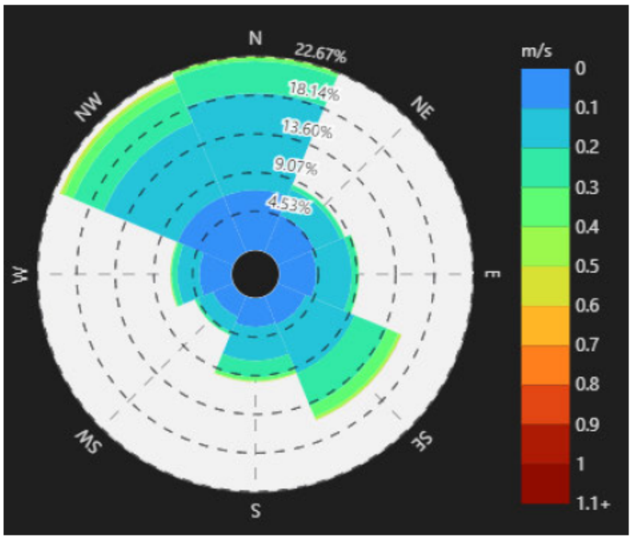

Figure 2-2 Current rose for the proposed locations of the mussel spat nursery Site A.

Table 2-5 Current speed (m/s) and current direction joint probability for the mussel nursery site B.

Current speed (m/s) / direction	**N**	**NE**	**E**	**SE**	**S**	**SW**	**W**	**NW**
0 - 0.1	7%	4.70%	4.30%	3.60%	3.40%	2.60%	3.70%	7%
0.1 - 0.2	11.40%	3.30%	4.10%	6.20%	3.90%	1.90%	2.60%	9.40%
0.2 - 0.3	3.70%	0.50%	0.80%	4.10%	1.90%	0.30%	0.60%	3.90%
0.3 - 0.4	0.40%	<0.1%	<0.1%	1.40%	0.40%	<0.1%	0.10%	1.20%
0.4 - 0.5	0.10%	<0.1%	<0.1%	0.30%	0.10%	0%	<0.1%	0.40%
0.5 - 0.6	<0.1%	0%	0%	<0.1%	<0.1%	0%	<0.1%	0.10%
0.6 - 0.7	0%	0%	0%	0%	<0.1%	0%	0%	<0.1%
0.7 - 0.8	0%	0%	0%	0%	0%	0%	0%	0%
0.8 - 0.9	0%	0%	0%	0%	0%	0%	0%	0%
0.9 - 1	0%	0%	0%	0%	0%	0%	0%	0%
1 - 1.1	0%	0%	0%	<0.1%	0%	0%	0%	0%

2.2 Site B

Wave data for Site B was extracted from the nearest model node at -37.64°S, 174.72°E, and current data from the nearest model node -37.6927°S, 174.6594°E. The predominant swell direction at Site B is from the SW (probability 79.0%) and significant wave heights from this direction most frequently range between 1.0 to 3.5 m (Table 2-6).

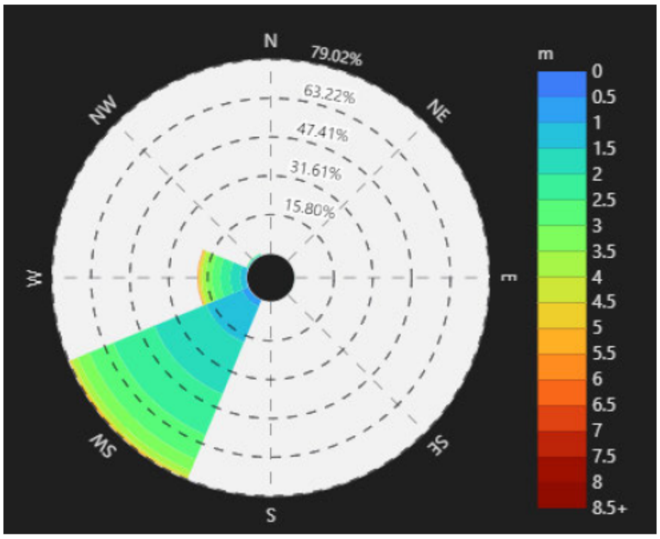

Figure 2-3 Wave rose for the proposed locations of the mussel spat nursery Site B.

Table 2-6 Significant wave height and mean direction of spectral peak joint probability (%) for mussel spat nursery Site A.

Wave height / Wave direction	N	NE	E	SE	S	SW	W	NW
0 - 0.5	0%	0%	0%	0%	0%	<0.1%	<0.1%	0%
0.5 - 1	0%	<0.1%	<0.1%	0%	<0.1%	2.80%	0.40%	<0.1%
1 - 1.5	0%	<0.1%	<0.1%	<0.1%	0%	15.90%	2.10%	0.20%
1.5 - 2	<0.1%	0%	<0.1%	<0.1%	<0.1%	22.80%	4.10%	0.30%
2 - 2.5	0%	0%	0%	0%	0%	17.90%	4.10%	0.30%
2.5 - 3	0%	0%	0%	0%	0%	10.70%	3.30%	<0.1%
3 - 3.5	0%	0%	0%	0%	0%	5.20%	2.40%	<0.1%
3.5 - 4	0%	0%	0%	0%	0%	2.30%	1.60%	<0.1%
4 - 4.5	0%	0%	0%	0%	0%	1%	0.90%	<0.1%
4.5 - 5	0%	0%	0%	0%	0%	0.40%	0.50%	0%
5 - 5.5	0%	0%	0%	0%	0%	0.20%	0.30%	0%
5.5 - 6	0%	0%	0%	0%	0%	<0.1%	0.10%	0%
6 - 6.5	0%	0%	0%	0%	0%	<0.1%	<0.1%	0%
6.5 - 7	0%	0%	0%	0%	0%	<0.1%	<0.1%	0%
7 - 7.5	0%	0%	0%	0%	0%	0%	<0.1%	0%
7.5 - 8	0%	0%	0%	0%	0%	0%	<0.1%	0%
8 - 8.5	0%	0%	0%	0%	0%	0%	<0.1%	0%

A joint probability analysis of significant wave height and relative peak period, shows higher probability of wave heights ranging between 1.0 and 3.5 m and 11 to 17 second periods (Table 2-7).

Table 2-7 Significant wave height (m) and relative peak period (smooth) joint probability (%) for mussel spat nursery Site A.

Wave height (m) \ Peak period	0 - 1	1-2	2-3	3-4	4-5	5-6	6-7	7-8	8-9	9-10	10-11	11-12	12-13	13 - 14	14 - 15	15 - 16	16 - 17	17 - 18	18 - 19	19 - 20
0 - 0.5	0	0	0	0	0	0	0	0	0	0	<0.1	<0.1	<0.1	<0.1	0	0	0	<0.1	<0.1	0
0.5 - 1	0	0	0	<0.1	<0.1	<0.1	<0.1	<0.1	<0.1	<0.1	0.20	0.60	0.90	0.60	0.30	0.20	0.20	<0.1	<0.1	<0.1
1 - 1.5	0	0	0	<0.1	<0.1	<0.1	0.10	0.20	0.20	0.30	0.70	2.50	4.50	4.30	2.30	1.30	1	0.30	0.40	0.10
1.5 - 2	0	0	0	0	<0.1	<0.1	0.20	0.40	0.60	0.70	1	2.40	5.10	6.80	4.50	2.60	1.80	0.50	0.50	0.20
2 - 2.5	0	0	0	0	0	0	0.10	0.40	0.70	0.70	1.10	1.60	3.10	5.10	4.40	2.60	1.70	0.40	0.30	0.10
2.5 - 3	0	0	0	0	0	0	<0.1	0.30	0.50	0.50	0.60	1	1.70	2.80	2.80	2.10	1.20	0.30	0.20	<0.1
3 - 3.5	0	0	0	0	0	0	0	<0.1	0.40	0.40	0.40	0.40	0.80	1.40	1.40	1.20	0.90	0.20	0.10	<0.1
3.5 - 4	0	0	0	0	0	0	0	<0.1	0.10	0.30	0.20	0.20	0.40	0.60	0.70	0.60	0.50	0.10	<0.1	<0.1
4 - 4.5	0	0	0	0	0	0	0	0	<0.1	0.10	0.20	0.10	0.20	0.30	0.30	0.30	0.20	<0.1	<0.1	<0.1
4.5 - 5	0	0	0	0	0	0	0	0	0	<0.1	0.10	<0.1	0.10	0.10	0.20	0.10	<0.1	<0.1	<0.1	<0.1
5 - 5.5	0	0	0	0	0	0	0	0	0	<0.1	<0.1	<0.1	<0.1	<0.1	<0.1	<0.1	<0.1	<0.1	<0.1	0
5.5 - 6	0	0	0	0	0	0	0	0	0	0	<0.1	<0.1	<0.1	<0.1	<0.1	<0.1	<0.1	<0.1	0	0
6 - 6.5	0	0	0	0	0	0	0	0	0	0	0	<0.1	<0.1	<0.1	<0.1	<0.1	<0.1	0	0	0
6.5 - 7	0	0	0	0	0	0	0	0	0	0	0	0	<0.1	<0.1	<0.1	<0.1	<0.1	0	0	0
7 - 7.5	0	0	0	0	0	0	0	0	0	0	0	0	0	<0.1	<0.1	0	<0.1	0	0	0
7.5 - 8	0	0	0	0	0	0	0	0	0	0	0	0	0	<0.1	<0.1	0	<0.1	0	0	0
8 - 8.5	0	0	0	0	0	0	0	0	0	0	0	0	0	0	0	<0.1	0	0	0	0

The 1=year return period significant have height is 7.1 m significant (Table 2-8).

Table 2-8 Extreme analysis of wave and wind conditions at Site B.

Return period [years]	1	5	10	50	100	1000	10000
Significant wave height (m)	7.1	7.8	8.2	8.9	9.2	10.3	11.4
Wind speed (m/s)	26.3	30.7	32.6	37.3	39.4	46.6	54.2

The predominant current direction at Site B is N (probability 35%, Figure 2-4), however, currents will swing between NW to S (Figure 2-4, Table 2-9).

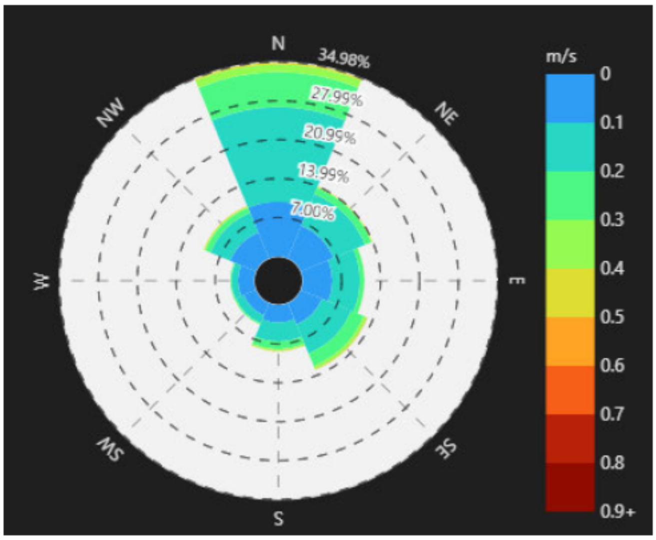

Figure 2-4 Current rose for the proposed locations of the mussel spat nursery Site B.

Table 2-9 Current speed (m/s) and current direction joint probability for the mussel nursery site B.

current speed (m/s) \ direction	N	NE	E	SE	S	SW	W	NW
0 - 0.1	9.80%	6.40%	5.30%	4.10%	3.10%	2.40%	2.90%	5%
0.1 - 0.2	17%	6.10%	4.90%	5.70%	3.40%	1.50%	1.20%	3.80%
0.2 - 0.3	6.30%	1.20%	0.80%	2.40%	1.40%	0.30%	0.20%	1%
0.3 - 0.4	1.40%	0.20%	<0.1%	0.60%	0.30%	<0.1%	<0.1%	0.20%
0.4 - 0.5	0.30%	<0.1%	0%	0.10%	<0.1%	0%	0%	0.10%
0.5 - 0.6	<0.1%	0%	0%	<0.1%	0%	0%	0%	0%
0.6 - 0.7	0%	0%	0%	0%	<0.1%	0%	0%	0%
0.7 - 0.8	0%	0%	0%	0%	0%	0%	0%	0%
0.8 - 0.9	0%	0%	0%	<0.1%	0%	0%	0%	0%

2.3 Site C

Wave data for Site C was extracted from the nearest model node at -37.68°S, 174.760°E, and current data from the nearest model node at -37.7076°S, 174.6927°E. The predominant swell direction here is from the SW and the most frequently encountered significant wave heights range between 1.5 to 2.0 m (23.3% probability, Table 2-10).

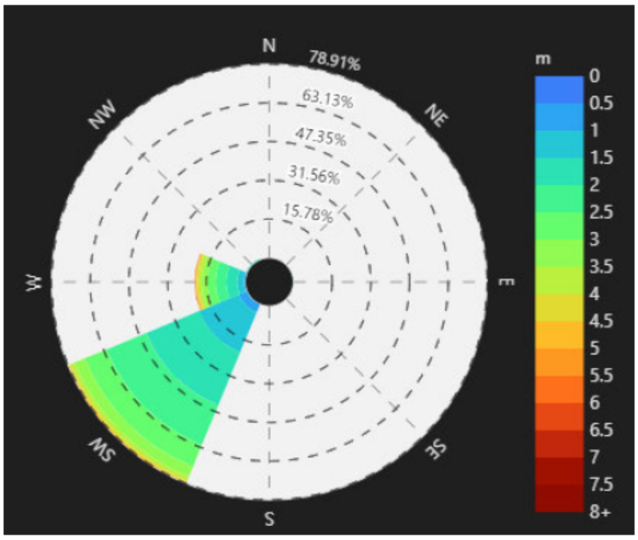

Figure 2-5 Wave rose for the proposed locations of the mussel spat nursery Site C.

Table 2-10 Wave height and direction joint probability for mussel spat nursery Site C.

Significant wave height (m) \ direction	N	NE	E	SE	S	SW	W	NW
0 - 0.5	0%	0%	0%	0%	0%	<0.1%	<0.1%	0%
0.5 - 1	0%	0%	<0.1%	0%	0%	3.50%	0.60%	<0.1%
1 - 1.5	0%	<0.1%	<0.1%	<0.1%	0%	17.70%	2.60%	0.10%
1.5 - 2	0%	0%	<0.1%	<0.1%	0%	23.30%	4.50%	0.20%
2 - 2.5	0%	0%	0%	0%	0%	17.50%	4.30%	0.10%
2.5 - 3	0%	0%	0%	0%	0%	9.60%	3.30%	<0.1%
3 - 3.5	0%	0%	0%	0%	0%	4.40%	2.30%	<0.1%
3.5 - 4	0%	0%	0%	0%	0%	1.80%	1.50%	<0.1%
4 - 4.5	0%	0%	0%	0%	0%	0.70%	0.80%	0%
4.5 - 5	0%	0%	0%	0%	0%	0.20%	0.40%	0%
5 - 5.5	0%	0%	0%	0%	0%	<0.1%	0.20%	0%
5.5 - 6	0%	0%	0%	0%	0%	<0.1%	<0.1%	0%
6 - 6.5	0%	0%	0%	0%	0%	<0.1%	<0.1%	0%
6.5 - 7	0%	0%	0%	0%	0%	0%	<0.1%	0%
7 - 7.5	0%	0%	0%	0%	0%	0%	<0.1%	0%
7.5 - 8	0%	0%	0%	0%	0%	0%	<0.1%	0%

A joint probability analysis of wave height and relative peak period found that most frequently encountered combination is for a significant wave heights of 1.5 – 2 m and 13-14 second periods (probability = 6.8%, Table 2-11). However, relative peak periods are mainly spread between 11 to 17 seconds.

Table 2-11 Significant wave height (m) and relative peak period (smooth) joint probability (%) for mussel spat nursery Site C.

Wave height \ Peak period	0 - 1	1-2	2-3	3-4	4-5	5-6	6-7	7-8	8-9	9-10	10-11	11-12	12-13	13 - 14	14 - 15	15 - 16	16 - 17	17 - 18	18 - 19	19 - 20
0 - 0.5	0	0	0	0	0	0	0	0	0	0	<0.1	<0.1	<0.1	<0.1	<0.1	0	0	<0.1	<0.1	0
0.5 - 1	0	0	0	<0.1	<0.1	<0.1	<0.1	<0.1	<0.1	<0.1	0.20	0.70	1.10	0.90	0.40	0.30	0.30	<0.1	<0.1	<0.1
1 - 1.5	0	0	0	<0.1	<0.1	<0.1	0.10	0.20	0.30	0.30	0.70	2.60	4.90	4.80	2.70	1.60	1.20	0.40	0.40	0.10
1.5 - 2	0	0	0	0	<0.1	<0.1	0.20	0.40	0.60	0.70	1.10	2.30	4.90	6.80	4.80	2.90	2	0.50	0.60	0.20
2 - 2.5	0	0	0	0	0	<0.1	<0.1	0.40	0.60	0.60	1	1.60	2.80	4.70	4.40	2.90	1.90	0.50	0.40	0.10
2.5 - 3	0	0	0	0	0	0	<0.1	0.20	0.50	0.50	0.60	0.90	1.50	2.50	2.60	2.10	1.30	0.30	0.20	<0.1
3 - 3.5	0	0	0	0	0	0	0	<0.1	0.30	0.40	0.30	0.40	0.70	1.10	1.10	1.10	0.90	0.20	0.10	<0.1
3.5 - 4	0	0	0	0	0	0	0	0	<0.1	0.20	0.20	0.20	0.30	0.50	0.60	0.50	0.50	0.10	<0.1	<0.1
4 - 4.5	0	0	0	0	0	0	0	0	<0.1	<0.1	0.10	0.10	0.20	0.20	0.30	0.20	0.20	<0.1	<0.1	<0.1
4.5 - 5	0	0	0	0	0	0	0	0	0	<0.1	<0.1	<0.1	<0.1	0.10	0.10	0.10	<0.1	<0.1	<0.1	0
5 - 5.5	0	0	0	0	0	0	0	0	0	0	<0.1	<0.1	<0.1	<0.1	<0.1	<0.1	<0.1	<0.1	<0.1	0
5.5 - 6	0	0	0	0	0	0	0	0	0	0	0	<0.1	<0.1	<0.1	<0.1	<0.1	<0.1	<0.1	0	0
6 - 6.5	0	0	0	0	0	0	0	0	0	0	0	<0.1	<0.1	<0.1	<0.1	<0.1	<0.1	0	0	0
6.5 - 7	0	0	0	0	0	0	0	0	0	0	0	0	<0.1	<0.1	<0.1	0	<0.1	0	0	0
7 - 7.5	0	0	0	0	0	0	0	0	0	0	0	0	0	<0.1	0	0	<0.1	0	0	0
7.5 - 8	0	0	0	0	0	0	0	0	0	0	0	0	0	0	<0.1	<0.1	0	0	0	0

The 1-year return period significant wave height is 6.7 m (Table 2-12),

Table 2-12 Extreme analysis of wave and wind conditions at Site C.

Return period [years]	1	5	10	50	100	1000	10000
Significant wave height (m)	6.7	7.4	7.7	8.4	8.8	9.8	10.8
Wind speed (m/s)	25.5	29.7	31.6	36	38	44.8	52

The predominant current direction is to the North at Site C (Figure 2-6 and Table 2-13).

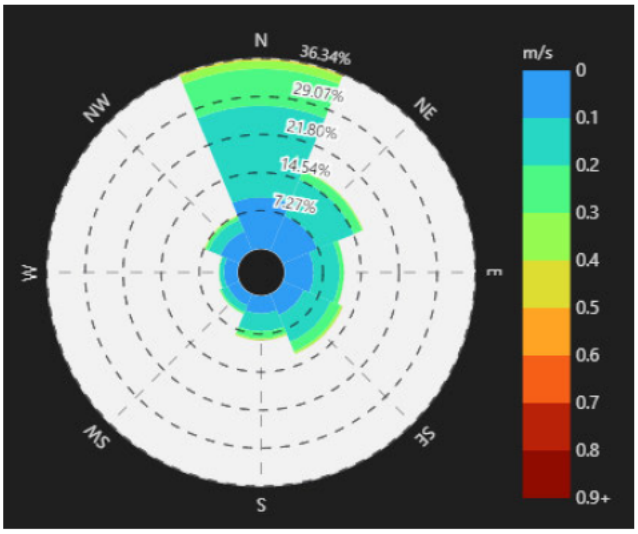

Figure 2-6 Current rose for the proposed locations of the mussel spat nursery Site C.

Table 2-13 Current speed (m/s) and current direction joint probability for the mussel nursery site C.

current speed (m/s) / direction	N	NE	E	SE	S	SW	W	NW
0 - 0.1	9.80%	7.20%	5.40%	4.30%	3.30%	2.30%	2.50%	4%
0.1 - 0.2	17.50%	7.50%	5%	5.60%	3.40%	1.40%	0.90%	2.40%
0.2 - 0.3	7.10%	1.70%	0.90%	2%	1.30%	0.30%	0.10%	0.70%
0.3 - 0.4	1.50%	0.20%	<0.1%	0.40%	0.30%	<0.1%	<0.1%	0.20%
0.4 - 0.5	0.30%	<0.1%	0%	0.10%	<0.1%	0%	0%	<0.1%
0.5 - 0.6	<0.1%	0%	0%	0%	0%	0%	0%	0%
0.6 - 0.7	0%	0%	0%	0%	<0.1%	0%	0%	0%
0.7 - 0.8	0%	0%	0%	0%	0%	0%	0%	0%
0.8 - 0.9	0%	0%	0%	<0.1%	0%	0%	0%	0%

2.4 Site D

Wave data was extracted from the nearest model node at -37.88°S, 174.72°E and current data from the nearest model node -37.9002°S, 174.6927°E. The predominant swell direction is from SW and W (Figure 2-7) with the most frequently encountered significant wave heights ranging between 1.5 to 2.0 m from the SW (16.70% probability, Table 2-14).

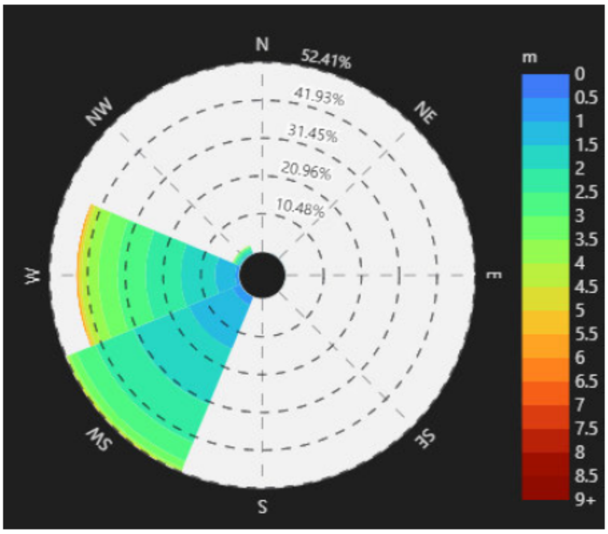

Figure 2-7 Wave rose for the proposed locations of the mussel spat nursery Site D.

Table 2-14 Wave height and direction joint probability for mussel spat nursery Site D.

Significant wave height (m) \ direction	N	NE	E	SE	S	SW	W	NW
0 - 0.5	0%	0%	0%	0%	0%	<0.1%	<0.1%	0%
0.5 - 1	0%	<0.1%	<0.1%	0%	0%	2.40%	1%	<0.1%
1 - 1.5	<0.1%	<0.1%	<0.1%	0%	0%	13.10%	5.50%	0.30%
1.5 - 2	<0.1%	<0.1%	<0.1%	<0.1%	0%	16.70%	9.50%	0.70%
2 - 2.5	0%	0%	0%	0%	0%	11.40%	9.80%	0.70%
2.5 - 3	0%	0%	0%	0%	0%	5.60%	7.70%	0.40%
3 - 3.5	0%	0%	0%	0%	0%	2.10%	5.30%	0.20%
3.5 - 4	0%	0%	0%	0%	0%	0.70%	3.10%	<0.1%
4 - 4.5	0%	0%	0%	0%	0%	0.20%	1.60%	<0.1%
4.5 - 5	0%	0%	0%	0%	0%	<0.1%	0.80%	<0.1%
5 - 5.5	0%	0%	0%	0%	0%	<0.1%	0.40%	<0.1%
5.5 - 6	0%	0%	0%	0%	0%	<0.1%	0.20%	<0.1%
6 - 6.5	0%	0%	0%	0%	0%	<0.1%	<0.1%	0%
6.5 - 7	0%	0%	0%	0%	0%	0%	<0.1%	0%
7 - 7.5	0%	0%	0%	0%	0%	0%	<0.1%	0%
7.5 - 8	0%	0%	0%	0%	0%	0%	<0.1%	0%
8 - 8.5	0%	0%	0%	0%	0%	0%	<0.1%	0%
8.5 - 9	0%	0%	0%	0%	0%	0%	<0.1%	0%

A joint probability analysis of wave height and relative peak period found that most frequently encountered combination is significant wave heights of 1.5 – 2.0 m and 13-14 second periods (probability = 6.8%, Table 2-15). However, relative peak periods mainly spread between 11 to 17 seconds.

Table 2-15 Significant wave height (m) and relative peak period joint probability (%) for mussel spat nursery Site D.

Significant wave height (m) \ Relative peak period (smooth) (sec)	0 - 1	1-2	2-3	3-4	4-5	5-6	6-7	7-8	8-9	9-10	10-11	11-12	12-13	13 - 14	14 - 15	15 - 16	16 - 17	17 - 18	18 - 19	19 - 20
0 - 0.5	0	0	0	0	0	0	0	0	0	0	<0.1	<0.1	<0.1	<0.1	0	0	0	<0.1	<0.1	0
0.5 - 1	0	0	0	<0.1	<0.1	<0.1	<0.1	<0.1	<0.1	<0.1	0.20	0.70	0.90	0.70	0.30	0.30	0.20	<0.1	<0.1	<0.1
1 - 1.5	0	0	0	<0.1	<0.1	<0.1	0.10	0.20	0.20	0.30	0.70	2.50	4.50	4.30	2.40	1.50	1.20	0.40	0.40	0.10
1.5 - 2	0	0	0	0	<0.1	<0.1	0.20	0.50	0.70	0.70	0.90	2.30	4.60	6.20	4.40	2.80	2.20	0.60	0.60	0.20
2 - 2.5	0	0	0	0	0	<0.1	0.10	0.60	0.80	0.80	1	1.50	2.60	4.40	4	2.90	2	0.50	0.40	0.20
2.5 - 3	0	0	0	0	0	0	<0.1	0.30	0.70	0.60	0.60	1	1.50	2.30	2.50	2.10	1.50	0.40	0.20	<0.1
3 - 3.5	0	0	0	0	0	0	0	<0.1	0.40	0.50	0.40	0.40	0.70	1.10	1.10	1.20	1	0.30	0.10	<0.1
3.5 - 4	0	0	0	0	0	0	0	<0.1	0.10	0.30	0.20	0.20	0.40	0.50	0.60	0.60	0.60	0.20	<0.1	<0.1
4 - 4.5	0	0	0	0	0	0	0	0	<0.1	0.10	0.20	0.10	0.20	0.30	0.30	0.30	0.30	0.10	<0.1	<0.1
4.5 - 5	0	0	0	0	0	0	0	0	0	<0.1	0.10	<0.1	<0.1	0.10	0.10	0.10	<0.1	<0.1	<0.1	0
5 - 5.5	0	0	0	0	0	0	0	0	0	<0.1	<0.1	<0.1	<0.1	<0.1	<0.1	<0.1	<0.1	<0.1	<0.1	0
5.5 - 6	0	0	0	0	0	0	0	0	0	0	<0.1	<0.1	<0.1	<0.1	<0.1	<0.1	<0.1	<0.1	<0.1	0
6 - 6.5	0	0	0	0	0	0	0	0	0	0	0	<0.1	<0.1	<0.1	<0.1	<0.1	<0.1	<0.1	0	0
6.5 - 7	0	0	0	0	0	0	0	0	0	0	0	<0.1	<0.1	<0.1	<0.1	<0.1	<0.1	0	0	0
7 - 7.5	0	0	0	0	0	0	0	0	0	0	0	0	<0.1	<0.1	<0.1	0	<0.1	0	0	0
7.5 - 8	0	0	0	0	0	0	0	0	0	0	0	0	0	<0.1	0	0	<0.1	0	0	0
8 - 8.5	0	0	0	0	0	0	0	0	0	0	0	0	0	0	<0.1	0	0	0	0	0
8.5 - 9	0	0	0	0	0	0	0	0	0	0	0	0	0	0	0	<0.1	0	0	0	0

The 1-year return period significant wave height is 7.1 m at site D (Table 2-16).

Table 2-16 Extreme analysis of wave and wind conditions at Site D.

Return period [years]	1	5	10	50	100	1000	10000
Significant wave height (m)	7.1	7.9	8.2	9	9.4	10.5	11.6
Wind speed (m/s)	23.4	25.7	26.6	28.8	29.7	32.8	35.7

The current at Site D predominantly flows to the N (probability= 35.0%) and NE (19.0%) and occasionally diverts toward E (10.0%), SE (11.9%) and S (10.0%).

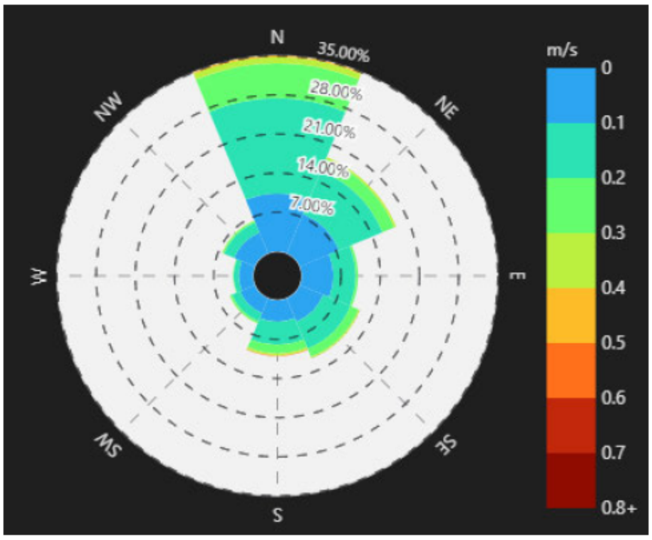

Figure 2-8 Current rose for the proposed locations of the mussel spat nursery Site C.

Table 2-17 Current speed (m/s) and current direction joint probability for the mussel nursery site C.

Current speed (m/s) / current direction	N	NE	E	SE	S	SW	W	NW
0 - 0.1	10.4%	7.6%	5.6%	4.5%	3.8%	2.8%	2.5%	4.0%
0.1 - 0.2	17.0%	8.4%	4.0%	5.3%	4.1%	1.6%	0.9%	2.0%
0.2 - 0.3	6.3%	2.3%	0.4%	1.6%	1.5%	0.4%	0.1%	0.3%
0.3 - 0.4	1.1%	0.4%	<0.1%	0.3%	0.4%	<0.1%	0.0%	<0.1%
0.4 - 0.5	0.2%	<0.1%	0.0%	<0.1%	<0.1%	0.0%	0.0%	0.0%
0.5 - 0.6	0.0%	0.0%	0.0%	0.0%	<0.1%	0.0%	0.0%	0.0%
0.6 - 0.7	0.0%	0.0%	0.0%	0.0%	0.0%	0.0%	0.0%	0.0%
0.7 - 0.8	0.0%	0.0%	0.0%	<0.1%	0.0%	0.0%	0.0%	0.0%

3. Assessment of potential environmental impacts

As discussed in Mascorda Cabre et al. 2021, large offshore aquaculture installations impact local hydrodynamics by acting as physical obstacles to water flow. As a porous structure, water flow blockage is partial, differing from the effects that other well-studied solid structures such as islands or sea defences (Plew et al. 2006; O'Donncha et al. 2013) by creating velocity shears and mixing layers and producing small-scale turbulence causing enhanced dispersion (see Figure 3-1; Plew et al. 2005, 2006; O'Donncha et al. 2013, 2016; Plew 2013; Matarazzo Suplicy 2018). The effects are closely related to the hydrodynamics and bathymetry of the area as well as the overall dimensions, extent, shape, and layout of the farm (orientation of the farm's structures to prevailing currents and waves and/or spacing between headlines) as well as the density of both the farm and the mussels on the ropes (farm's canopy).

A collection of elements that form a porous obstacle to water flow can be described as canopies. When a suspended canopy extends a few metres downwards below the water surface, this can also be referred to as submerged canopy such as those created by submerged longline mussel farms (Plew et al. 2006).

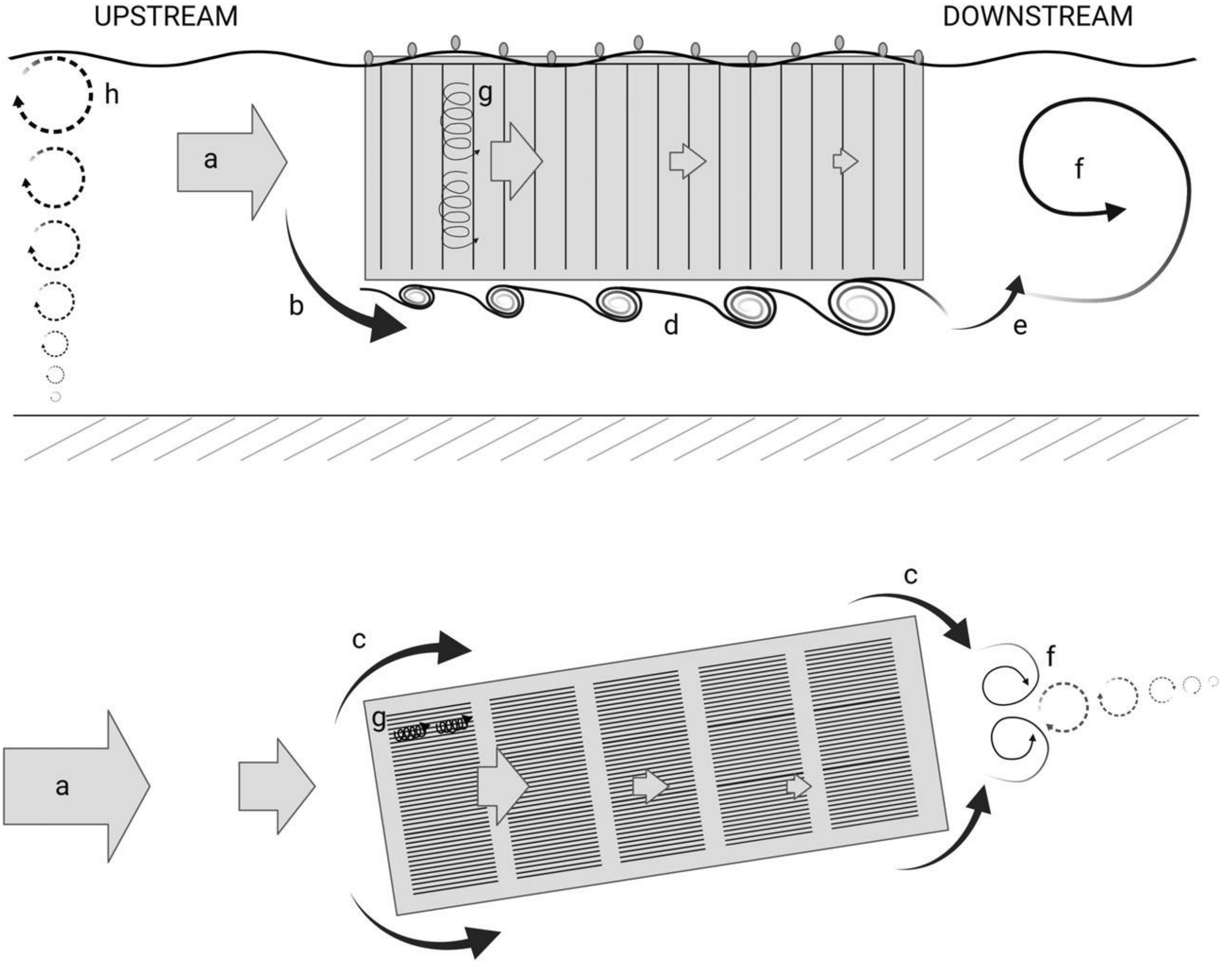

Figure 3-1: Elevation (top) and plan views (bottom) of an offshore longline mussel farm indicating various potential hydrodynamic processes: (a) waterflow and current attenuation, (b) downwelling, (c) corner acceleration, (d) accelerating undercurrent mixing layer, (e) upwelling, (f) recirculating zone, vortex or wake formation downstream of the farm, (g) turbulence within mussel longlines and (h) waves. The figure exemplifies one of many designs that could be attributed to offshore longline mussel farm's constantly evolving outlines (Graphic Mascorda Cabre 2020 created with BioRender.com, adapted from Plew et al. 2005).

3.1 Potential effects on incident wave climate

During wave attenuation, energy is transferred from the wave field to turbulence as the waves propagate through a canopy. Although wave-driven flexible structures such as a longline mussel farms, move and flex to accommodate this transfer of energy, such drag-induced water flow velocity modifications have been detected within suspended aquaculture structures (Plew et al. 2005).

Plew et al. (2005) found that the wave height attenuation associated with mussel farms is predominantly frequency dependent and to a lesser extent dependant on the incident wave height, with attenuation increasing for waves of larger amplitude (Figure 3-2). As such, Plew et al. (2005) described an average 10% decrease in wave amplitudes for incident wave conditions with peak periods of 7 seconds or less. In contrast, wave amplitudes for incident waves with peak periods of 7 to 10 seconds, were only reduced by an average of 5%.

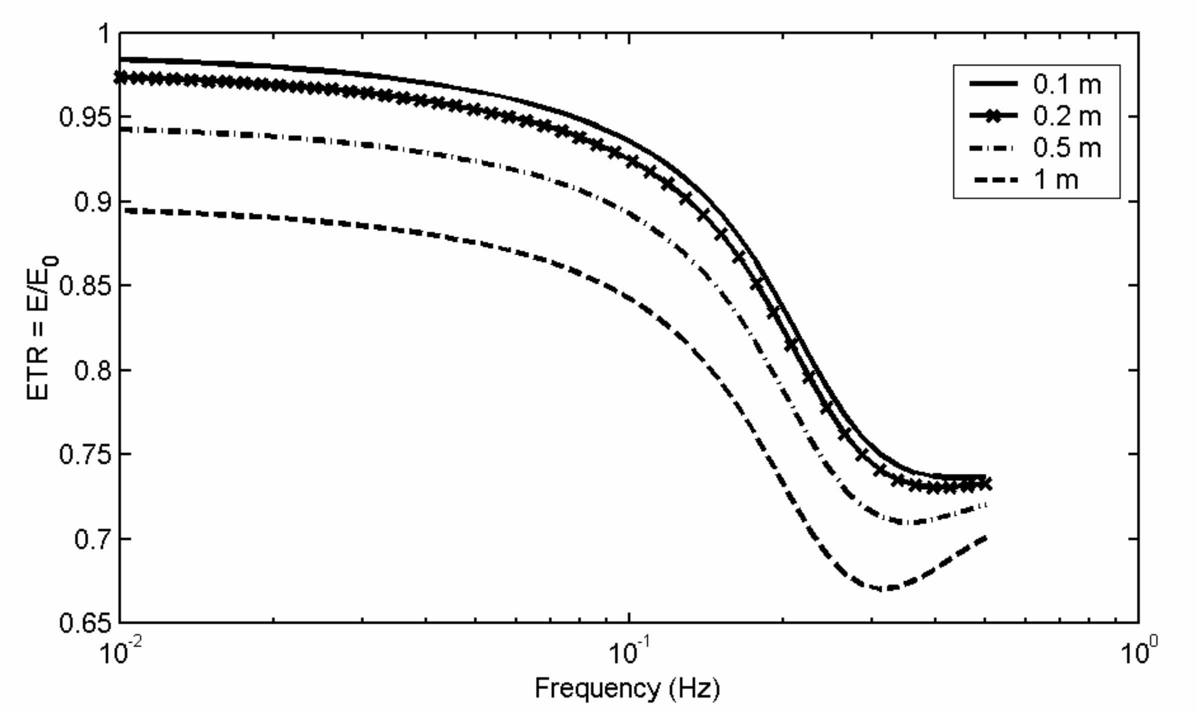

Figure 3-2: Energy transmission ratio (ETR) from wave model as function of initial wave height. Extracted from Plew et al. (2005), Figure 5.2.

Peak wave periods at the four proposed spat nursery sites of the coast of Raglan, range most frequently between 11 to 17 seconds (Section 2) and based on the finding of Plew et al. (2005) the wave climate may therefore be less impacted than a site dominated by shorter peak period (T<10s, i.e., higher frequencies > 0.1Hz). However, it is noted that the study from Golden Bay was conducted at a time of low wave energy (significant wave heights up to 0.25 m) and Plew et al. (2005) are, therefore, not confident on the accuracy of their empirical relationship at higher wave heights than those measured.

In addition to wave frequency and amplitude, Plew et al. (2005) stated that the impact of a mussel farm on wave climate is also dependency on the dropper line density as well as the size and orientation of the farm. Furthermore, the energy dissipation increases with distance from the farm, and with dropper density as shown on Figure 3-3.

The large mussel farm studied by Plew et al. (2005) covers an area of almost 160 ha (2450 m by 650 m) with 230 long-lines and a dropper density of 0.06 m^{-2}. The study considered a dropper with mature mussels (harvest size of 80mm to 150mm) which led to a conservative estimate of the velocity attenuation.

The proposed mussel spat operations of the coast of Raglan will consist of longlines spaced 50 metres apart i.e., with 41 longlines per row, covering areas of 160 to 180 ha (Table 1-1) resulting in dropper densities ranging from 0.04 to 0.08 dropper.m^{-2} (see Section 1.2). Considering the dropper density of the large mussel farm in Golden Bay studied by Plew et al. 2005 (0.06 dropper.m^{-2}) and that of the that the proposed spat nursery sites (0.04-0.08 dropper.m^{-2}, it is reasonable to assume that the proposed spat nursery sites will have similar or less impacts on the incident wave climates noting that the spat size will be much smaller than mature mussels. The wave energy transmission (or wave energy loss) through the 2000m spat nursery site for a dropper density of 0.04-0.08 dropper. m^{-2} is expected to be about 0.80 to 0.65 that is to 20-35% of the wave energy is absorbed by the spat nursery (see Figure 3-3) . These values are highly conservative due to the size of the spat compared a mature mussel farm used for this study. Nevertheless it is expected that the spat farm will attenuate some of the wave energy locally.

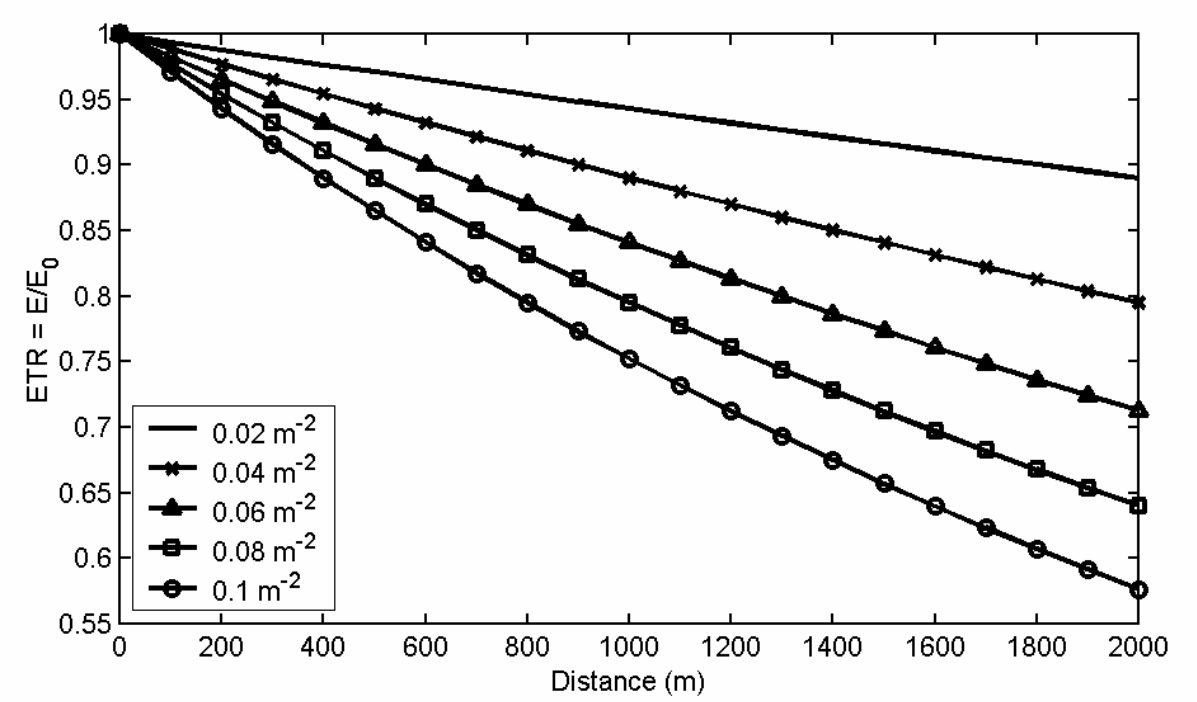

Figure 3-3: Energy Transmission Ratio (ETR) as a function of distance and dropper density (from Plew et al 2005 Figure 5.1)

3.2 Potential effects on current attenuation

As longline mussel farms do not extend over the full water depth, flow diversion is expected to be both vertically and horizontally around the canopy. Studies have identified that a main factor key to water flow modification is the angle of inference between upstream longlines and water flow (Mascorda Carbe et al. 2021). Longlines aligned with the water flow only allow little water flow to pass thereby reducing the velocity significantly (Delaux et al. 2011) and creating vorticity within and in the lee of the farms. In contrast, longlines installed perpendicular to the current flow results in an even spread and thus less vorticity.

Plew et al. (2006) found that an angle of 45 degrees between longlines and water flow resulted in the best farm performance. Whereas work by Delaux et al. (2011) based on a 2D high resolution computational fluid dynamics model, suggested angles of 50 to 90 degrees rendered the best results. The rows of the proposed spat nursery sites are orientated perpendicularly (< 90 degrees) to predominant current flow (Figure 3-1), and the longlines are oriented parallel (i.e., running along the width of the rows), and thus, based on the existing literature (Plew et al. 2006, Delaux et al. 2011), the impact on current attenuation is likely to be minimised.

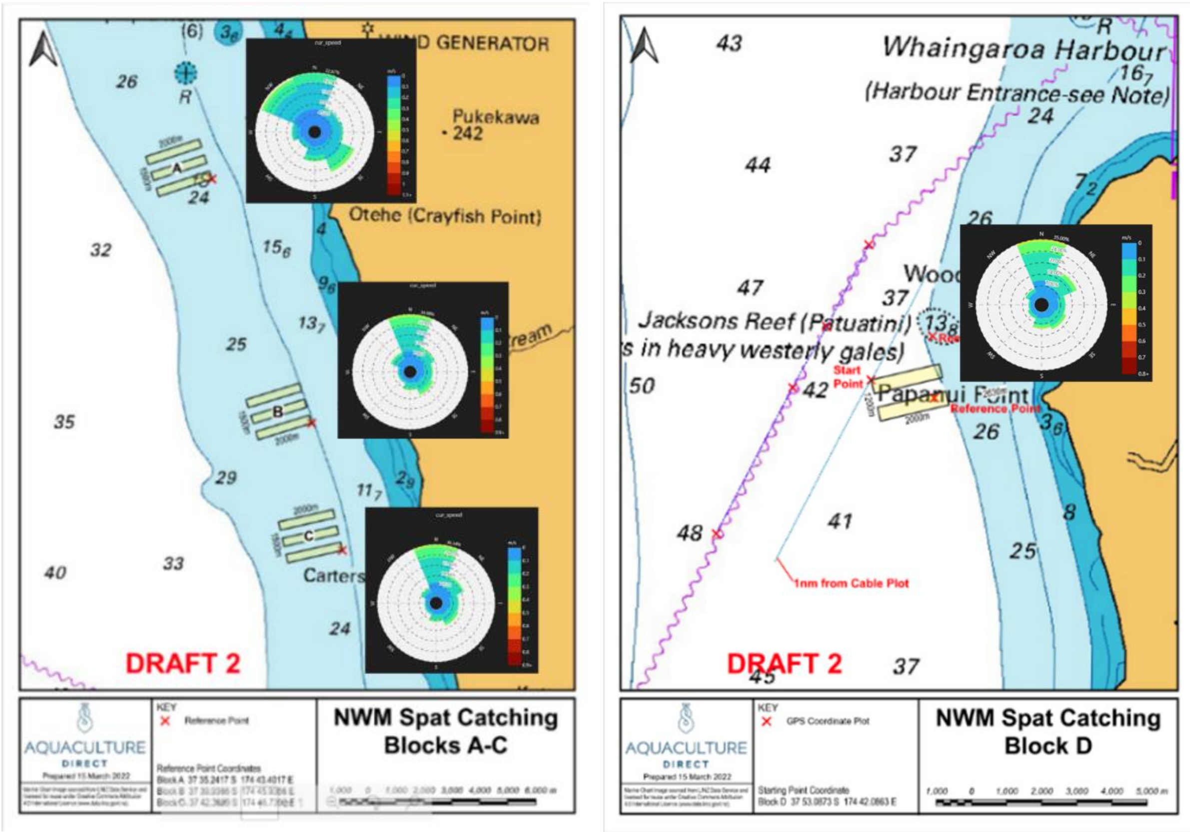

Figure 3-4. Directional orientations of the rows/longlines, and current roses (based on 30 year hindcast) at Site A, B, C and D of the proposed spat nursery operation of the coast of Raglan.

In contrast to other submerged canopies, mussel lines do not extend to the surface or the sea floor but are rather suspended in the water column (Mascorda Carbe et al. 2021), and field studies imply that water flows are diverted both under and around marine farms (Plew et al. 2005; Rampazzo et al. 2013; Lin et al. 2016). Plew (2005) and Plew et al. (2006) noted that when the gap between the dropper line and the seabed decreases, it restricts the vertical flow diversion and the current velocity underneath the farm increases. If the gap between the bottom of the dropper line and seafloor is less than 10 to 30% of the total water column, the flow is likely to be restricted (Plew et al. 2006). At the proposed spat nursery sites, the gap between the dropper lines (8 m depth) and the sea floor (20 to 40 m depth) is planned to be >60% of the total water column, thus the impact on the vertical flow diversion is likely minimal.

Current attenuation inside marine farms have been found to be reduced by 75% and up to 90% in extreme cases (Plew 2013; Lin et al. 2016; Hulot et al. 2018; Zhong et al. 2022). However, the impact on the current velocity may not be restricted to the farm as the submerged canopies may form a wake, an area of reduced current velocities downstream of the farm (Plew 2005, Delaux 2011). As such, Plew (2005) detected significant changes in the current velocities up to 100 m from the nearest longline. In contrast, an earlier study of a small farm of only 8-10 longlines described in Waite (1989) and Gibbs et al.

(1991), found little effect on current velocities beyond the farm. Nevertheless, it is expected that a wake (i.e. turbulence, reduction of mean flow..) will develop in the lee of the farm. Plew (2005) noted that the farm wake may have a nearly constant velocity across its width, but as the wake spreads downstream, it will develop a Gaussian profile typical of the far wakes of bluff bodies. In a tidal environment the extent of the wake is expected to be similar to the tidal excusion. For the Golden Bay mussel farm , the furthest point of the wake detected was approximately 2.4km for the

Plew (2005) presents a correlation for the reduction in current velocities based on a range of dropper densities, with the dropper density from 0.01 to 0.1 m^2 (see Figure 3-5). The Golden Bay mussel farm studied by Plew 2005, has a dropper line density of 0.06 dropper.m^{-2}, which is in the same order of magnitude to the conditions proposed in the Raglan nursery application (0.04 to 0.08 dropper.m^{-2}) considering that the spats are also much smaller in size than mature mussels . The downstream velocity decays downstream of the proposed nursery sites are, therefore, likely to be similar or less than the Golden Bay farm noting that the proposed spat farm is also in much deeper water Due to the orientation of the currents at the sites, the farm wakes are expected to be in a north-northwest and south-southeast direction for all sites and depending on their potentially interacting for block A, B and C.

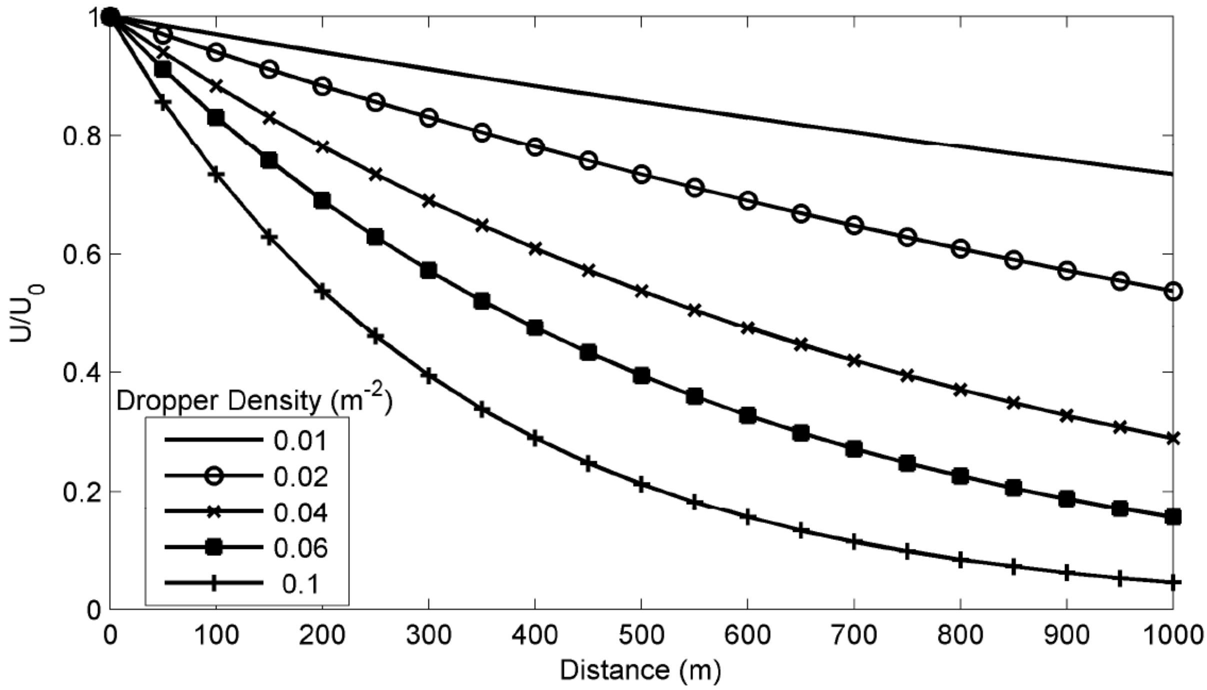

Figure 3-5: Analytical prediction for velocity decay through farm. A range of mussel dropper densities (droppers per m^2) are shown (Source: Figure 3.17 in Plew 2005).

Drag is a function of longline orientation, line density and spacing (Mascorda Carbe et al. 2021). Given that the density of spat nursery lines and associated line roughness are expected to be several orders of magnitude less than an operational mussel farm, the impacts of the proposed spat nursery aquaculture activities are expected to be localised and minor with respect to currents/hydrodynamics and hence no significant impact on the dynamic equilibrium of any beach within the environs or the movement of any detritus.

3.3 Potential effects on adjoining foreshore

Given the less than minor impact of the proposed spat farms on both the incident wave climate and currents (Section 3.1 and 3.2), and the distance of the proposed farms to the shore (between three to four km), the impacts on coastal processes along the adjoining foreshore are likely to be minor.

3.4 Potential effects on national and regional surf breaks

There are four surf breaks of national significant in Waikato, (New Zealand Coastal Policy Statement (NZCPS), 2010), three of which are in Raglan. These are Manu Bay, Whale Bay, and Indicators, and collectively termed "the Points" (Atkin and Mead, 2016). Local governments are required by the NZCPS (2010) to protects surf breaks of national significance. The optimum swell direction for all three surf breaks is SW, (Atkin & Mead, 2016). One could argue that Site D is in the indirect swell corridor of these sites as the SW swell generating good surf conditions wraps around the headland created by Mount Karioi. The distances of Site D to the nearest of the Points, Indicators is approx. 11 km (Figure 3-6).

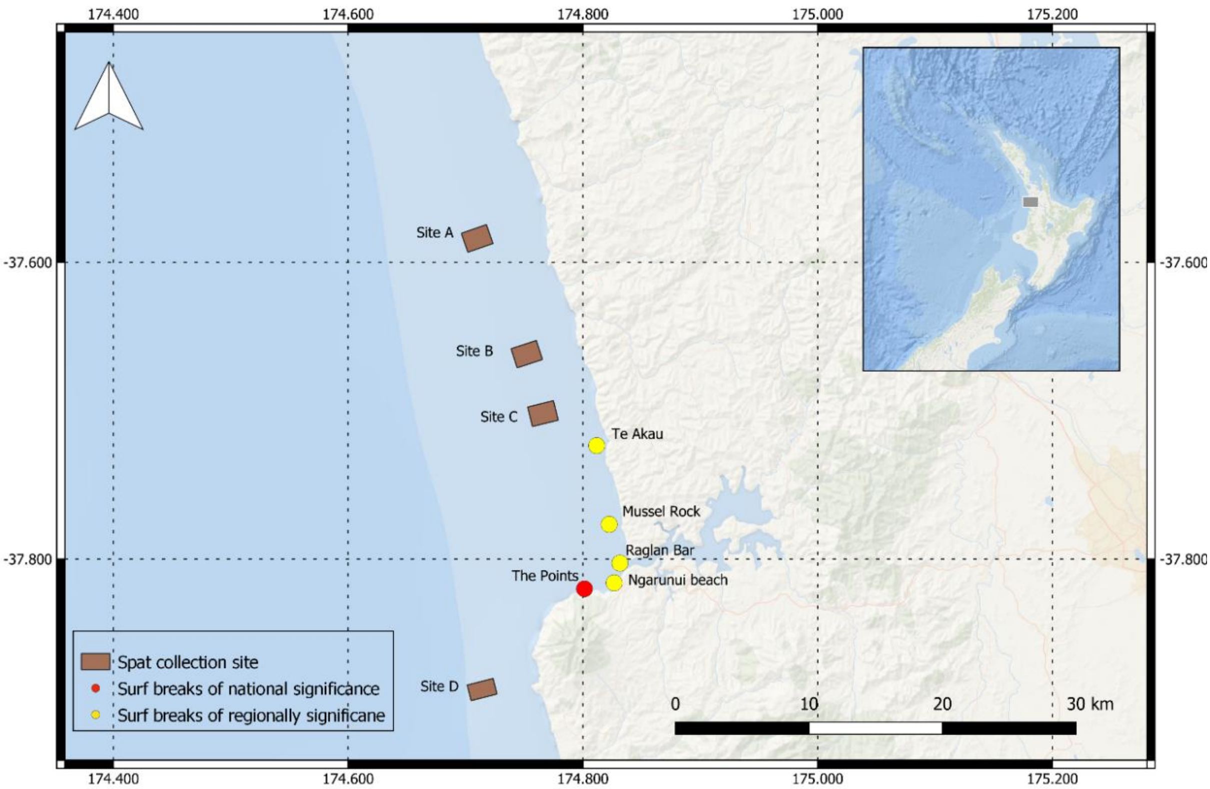

Figure 3-6 Map of surf breaks of national and regional significance (yellow and red points respectively) and proposed mussel spat nursery sites

A further four surf breaks of regional significance, as defined by Atkin and Mead (2017), are located along the coastline of the proposed sites (Figure 3-6). The optimum swell direction for the four surf breaks of regional significance; “Ngarunui Beach”, “Raglan Bar”, “Mussel Rock” and “Te Akau”, is SW (Atkin and Mead 2017). As such, at times of optimal swell conditions, Site D is in the distant (> 14.5 km) and indirect swell corridor (SSW) of the surf breaks (Figure 3).

It is likely that there are other surf spots of lesser significance along the shoreline in closer proximity to the nursery sites, however, these will be at least three km from the mussel nursery sites given the distance to shore. Given the dropper line density of the proposed spat nursery sites, as well as the greater distances from the sites to the surf break, these are unlikely to have significant impacts on either nationally or regionally significant surf breaks on the Waikato west coast. It should be noted that even though the impact is expected to be minimal, Site D is likely to receive the most attention regarding surf breaks. Further work would be needed to fully demonstrate the potential impact even if minimal.

4. Conclusions

The four proposed mussel spat nursery sites are based in wave climates prevailed by wave directions from SW and significant wave heights most frequently ranging between 1 to 3 metres with frequencies mostly ranging between 11 to 17 seconds (Section 2). Currents predominantly flow north and south and proposed long-lines of the nursery sites are therefore angled parallel to the predominant waterflow (Section 2).

The impacts of the proposed mussel nursery on both the incident wave climate and hydrodynamic conditions as discussed in Section 3. Given the dropper line density and angle to the predominant current flow, the proposed operations are likely to have some impacts on wave energy transfers and current velocity within the nursery. Further away from the nursery the impacts are expected to be minimal or negligible at the coast. Overall, based on the available information, it is likely that the hydrodynamic impacts of the proposal will be no more than minor.

Given the limited number of relevant studies to draw conclusive evidence from, further work is recommended as the proposal progresses, to ensure that impacts on the natural state of the environment, including on surf breaks of regional or national significance, at the nursery sites and at any distance from the nursery sites, are well understood.

Note:

As Site D is likely to receive the most attention, considering that it is located within the swell corridor of nationally or regionally significant surf breaks on the Waikato west coast, It might be prudent to assess the potential effect of wave attenuation away from the spat farm. Numerical wave modelling tests can be undertaken to demonstrate the wave attenuation potential at Site D and its effect on wave propagation towards the surf breaks.

An additional aspect that can also be discussed during the preparation of evidence is the deployment of a couple of wave buoys near the site as part of an adaptive management framework.

5.References

Ardhuin, F., Rogers,E., Babanin, A.V., Filipot, J.F., Magne, R., Roland, A., Van Der Westhuysen, A., Queffeulou, P., Lefevre, J.M., Aouf, L., Collard, F., 2010. Semiempirical dissipation source functions for ocean waves. Part I: Definition, calibration, and validation. Journal of Physical Oceanography 40, 1917–1941.

Atkin, E. and Mead, S.T., 2017. “Surf breaks of regional significance in the Waikato region”. Prepared for Waikato Regional Council.

Battjes, J.A., Janssen, J., 1978. Energy loss and set-up due to breaking of random waves. Coastal Engineering Proceedings 1.

Booij, N., Ris, R.C., Holthuijsen, L.H., 1999. A third-generation wave model for coastal regions: 1. Model description and validation. Journal of geophysical research: Oceans 104, 7649–7666.

Collins, J., 1972. Prediction of Shallow Water Spectra. Journal of Geophysical Research 77, 2693–2707.

Delaux S., Stevens C.L., and Popinetl S., 2011. “High-resolution computational fluid dynamics modelling of suspended shellfish structures.” *Environmental Fluid Mechanics* 11: 405–425

Gibbs, M. M., M. R. James, S. E. Pickmere, P. H. Woods, B. S. Shakespeare, R. W. Hickman and J. Illingworth (1991). "Hydrodynamic and water column properties at six stations associated with mussel farming in Pelorus Sound, 1984-85." *New Zealand Journal of Marine and Freshwater Research* 25: 239- 254.

Holthuijsen, L.H., Booij, N., Ris, R.C., Haagsma, I.J., Kieftenburg, A.T.M.M., Kriezi, E.E., Zijlema, M., van der Westhuysen, A.J., 2007. SWAN cycle III version 40.51, Technical Documentation. Delft, 2600 GA Delft The Netherlands.

Hulot V., Saulnier D., Lafabrie C., and Gaertner-Mazouni N., 2018. Shellfish culture: a complex driver of planktonic communities. *Reviews in Aquaculture* 12: 33–46

Lin J., Li C., and Zhang S., 2016. “Hydrodynamic effect of a large off-shore mussel suspended aquaculture farm”. *Aquaculture* 451: 147–155.

Mascorda Cabre, L., Hosegood, P., Attrill, M.J., Bridger, D., and Sheehan, E.V. 2021, “Offshore longline mussel farms: a review of oceanographic and ecological interactions to inform future research needs, policy and management.” *Reviews in Aquaculture* 13: 1864-1887. https://doi.org/10.1111/raq.12549

Plew, D.R., 2005. “The hydrodynamic effects of longline mussel farms”. PhD thesis, *University of Canterbury, Civil Engineering*.

Plew, D.R., Stevens, C.L., Spigel, R.H. and Hartstein, N.D., 2005. “Hydrodynamic implications of large offshore mussel farms.” *IEEE Journal of Oceanic Engineering*, 30(1), pp.95-108.

Plew, D. R., Spigel, R. H., Stevens, C. L., Nokes, R. I., Davidson, M.J., 2006. “Stratified flow interactions with a suspended canopy.” *Environmental Fluid Mechanics* 6: 519–539

Plew DR., 2013. “Hydrodynamic effects”. In Knight B (ed.), *Literature Review of Ecological Effects of Aquaculture*, pp. 11.1–11.23. Ministry for Primary Industries, Cawthron Institute & National Institute for Water and Atmospheric Research Ltd, New Zealand.

Rampazzo, F., Berto, D., Giani, M., Brigolin, D., Covelli, S., Cacciatore, F., ... & Pastres, R. 2013. “Impact of mussel farming on sedimentary geochemical properties of a Northern Adriatic area influenced by freshwater inflows”. *Estuarine, Coastal and Shelf Science*, 129, 49-58.

Rogers, W.E., Babanin, A.V., Wang, D.W., 2012. Observation-consistent input and whitecapping dissipation in a model for wind-generated surface waves: Description and simple calculations. Journal of Atmospheric and Oceanic Technology 29, 1329–1346.

Saha, S., Moorthi, S., Pan, H.-L., Wu, X., Wang, Jiande, Nadiga, S., Tripp, P., Kistler, R., Woollen, J., Behringer, D., Liu, H., Stokes, D., Grumbine, R., Gayno, G., Wang, Jun, Hou, Y.-T., Chuang, H.-Y., Juang, H.-M.H., Sela, J., Iredell, M., Treadon, R., Kleist, D., Van Delst, P., Keyser, D., Derber, J., Ek, M., Meng, J., Wei, H., Yang, R., Lord, S., Van Den Dool, H., Kumar, A., Wang, W., Long, C., Chelliah, M., Xue, Y., Huang, B., Schemm, J.-K., Ebisuzaki, W., Lin, R., Xie, P., Chen, M., Zhou, S., Higgins, W., Zou, C.-Z., Liu, Q., Chen, Y., Han, Y., Cucurull, L., Reynolds, R.W., Rutledge, G., Goldberg, M., 2010. The NCEP Climate Forecast System Reanalysis. Bull. Amer. Meteor. Soc. 91, 1015–1057. https://doi.org/10.1175/2010BAMS3001.1

Tolman, H.L., 1991. A Third-Generation Model for Wind Waves on Slowly Varying, Unsteady, and Inhomogeneous Depths and Currents. J. Phys. Oceanogr. 21, 782–797. https://doi.org/10.1175/1520-0485(1991)021<0782:ATGMFW>2.0.CO;2

Tseung, H.L., Kikkert, G.A., & Plew, D., 2016. “Hydrodynamics of suspended canopies with limited length and width”. *Environmental fluid Mechanics* **16**, 145–166 (2016). https://doi.org/10.1007/s10652-015-9419-y.

Waite, R. P., 1989. “The nutritional biology of *Pena canaliculus* with special reference to intensive mariculture systems.” Zoology. Christchurch, University of Canterbury: 136.

Zhong, W., Lin, J., Zou, Q., Wen, Y., Yang, W. and Yang, G., 2022. “Hydrodynamic effects of large-scale suspended mussel farms: Field observations and numerical simulations”. *Frontiers in Marine Science*, *9*, p.973155.

6. Appendix A: Metocean datasources

6.1 Atmospheric data

The 10-min averaged wind data at 10-m elevation and atmospheric pressure were prescribed by a regional atmospheric hindcast carried out by MetOcean Solutions from 1979-2019 (inclusive). The WRF (Weather Research and Forecasting) model was established over all New Zealand at hourly intervals and approximately 12 km resolution with a nested domain over central regions at 4 km resolution, including the Cook Strait. The hindcast was specifically tuned to provide highly accurate marine wind fields for metocean studies around New Zealand.

The WRF model boundaries were sourced from the CFSR (Climate Forecast System Reanalysis) dataset distributed by NOAA (Saha et al., 2010).

6.2 Wave data

The long-term hindcast wave modelling was performed using a modified version of Simulating WAve Nearshore (SWAN)[1]. This section describes details of the wave model and the technique employed in the simulations.

SWAN is a third generation ocean wave propagation model which solves the spectral action density balance equation (Booij et al., 1999). The model simulates the growth, refraction and decay of each frequency-direction component of the complete sea state, providing a realistic description of the wave field as it changes in time and space. Physical processes that can be modelled include the generation of waves by surface wind, dissipation by white-capping, resonant nonlinear interaction between the wave components, bottom friction and depth-induced wave breaking dissipation. A detailed description of the model equations, parametrisations and numerical schemes can be found in Holthuijsen et al. (2007) and in the SWAN documentation[2].

The wave hindcast was selected from a 10-year period, from 2010 to 2019. The model was configured in non-stationary mode including all third-generation physics. The ST6 configuration (Rogers et al., 2012) and the bottom friction scheme of Collins (1972) with coefficient of 0.015 were applied. Depth-induced wave breaking dissipation was modelled according to Battjes and Janssen (1978). The wave spectra were discretised with 36

[1] Modified from SWAN version of the 40.91 release
[2] http://swanmodel.sourceforge.net/

directional bins (10 deg directional resolution) and up to 41 frequencies logarithmically spaced between 0.041 and 1.864 Hz at 10% increments.

A dynamical downscaling nesting approach was applied to resolve the regional North Island area, with a regular SWAN nest with resolutions of ~4 km.

Full spectral boundaries for the parent SWAN hindcast domain were prescribed from a global implementation of the WAVEWATCHIII (WW3) spectral wave model (Tolman, 1991), run at 0.5 deg resolution with the source terms of Ardhuin et al. (2010).

The model was forced with surface winds from a configuration of the Weather Research and Forecasting (WRF) as described in the previous subsection.

6.3 Current data

The hindcast current data was extracted from the Moana Backbone data set. The hindcast dataset has hourly outputs over a 27-year period, from 1993 to 2020.

The Moana Backbone model is a 25+ years 3D hydrodynamic hindcast for New Zealand waters which consists of a high-resolution 3D ROMS model with outputs calibrated and validated against field data available around New Zealand. The ROMS spatial resolution is approximately 5x5 km and include the whole New Zealand (Figure 6-1). The ROMS model was run in three-dimensional mode and was nested within the he global GLORYS/Mercator reanalysis 12v1 (latest version from Nov 2018) at daily intervals and 8 km spatial resolution (Ferry et al., 2012). The atmospheric forcings were sourced from the CFSR reanalysis (Saha et al. 2010). Spectral tidal forcings were imposed at the ROMS domain boundaries by the Oregon State University Tidal Inverse Solution (OTIS), widely used to force regional and coastal domains in hydrodynamic models (Egbert and Erofeeva, 2002). A total of 11 tidal constituents were used.

The full dataset can be downloaded from the project webpage at https://www.moanaproject.org/. Model results are available as hourly and daily average values for temperature, salinity, velocity (u, v, w), and sea surface elevation.

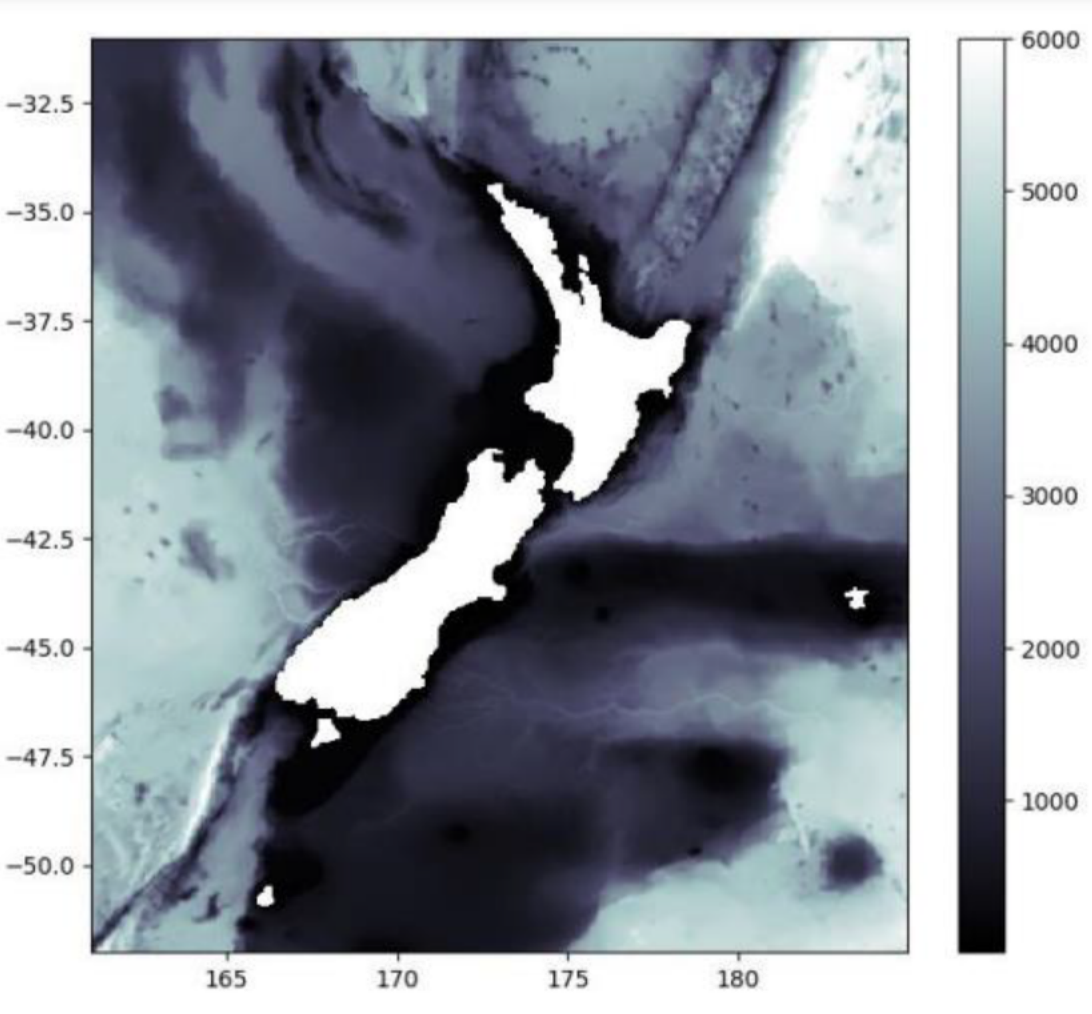

Figure 6-1 *Bathymetry map showing the extents of the hydrodynamic regional ROMS 3D domain at approximately 5 by 5 km resolution.*

7.Appendix B: Analytical methods

7.1 Wave parameters

The wave spectra were post-processed to calculate wave statistics for the total wave field. One-dimensional frequency spectra were defined by integrating over all directions:

$$E(f) = \int_{-\pi}^{\pi} E(f,\theta)d\theta. \tag{7.1}$$

Spectral moments were calculated as

$$m_x = \iint f^x E(f,\theta)df\,d\theta, \tag{7.2}$$

The significant wave height, H_s, mean direction at peak energy, Dpm, and peak wave period, T_p, are defined as:

$$H_s = 4\sqrt{m_0}, \tag{7.3}$$

$$Dpm = \tan^{-1}\frac{\int_{-\pi}^{\pi} E(f_p,\theta)\sin\theta\,d\theta}{\int_{-\pi}^{\pi} E(f_p,\theta)\cos\theta\,d\theta}, \tag{7.4}$$

$$T_p = 1/f_p, \tag{7.5}$$

where f_p is the peak wave frequency of the one-dimensional spectra and $E(f_p,\theta)$ is the energy contained in the peak wave frequency band.

7.2 Extreme value analysis

Return period values have been calculated from the hindcast time series of wind speed and significant wave height.

A *Peaks over Threshold* (POT) sampling method is used for event selection, applying the 95th percentile exceedance level as the threshold with a 24-hour window for omni-directional extremes. The selected wind events were fitted to a Weibull distribution, while H_s storm events were fitted to a generalised Pareto distribution, both with the location parameter fixed by the threshold and the Maximum Likelihood Method (MLM) used to obtain the scale and shape parameters.